AUDITORY TEMPORAL ACUITY AND ACROSS-FREQUENCY TEMPORAL PROCESSING

By

DAVID A. EDDINS

A DISSERTATION PRESENTED TO THE GRADUATE SCHOOL
OF THE UNIVERSITY OF FLORIDA IN PARTIAL FULFILLMENT
OF THE REQUIREMENTS FOR THE DEGREE OF
DOCTOR OF PHILOSOPHY

UNIVERSITY OF FLORIDA

1993

ACKNOWLEDGEMENTS

I gratefully acknowledge the support, guidance, and assistance of my advisor, Professor David M. Green. In sharing his kindness, wisdom, and knowledge, he has influenced my professional life in untold ways.

I also express my appreciation to the other members of my committee for their interest in my research and for their helpful comments. I truly thank all of those associated with the Psychoacoustics Laboratory for providing a wonderful atmosphere for learning and research. A special thanks goes to Dr. Beverly A. Wright for her cooperation and many helpful discussions.

Drs. Joseph W. Hall, John H. Grose, and Robert W. Peters inspired me to pursue auditory research and taught me many of the basic skills necessary to become a successful scientist. To them I will always be indebted.

I thank my parents for instilling in me an appreciation for knowledge and a drive to learn.

Finally, I wish to thank Dr. Ann E. Clock for her constant patience, support, and assistance during my doctoral training.

TABLE OF CONTENTS

Abstract of Dissertation Presented to the Graduate School of the University of Florida in Partial Fulfillment of the Requirements for the Degree of Doctor of Philosophy

AUDITORY TEMPORAL ACUITY AND ACROSS-FREQUENCY TEMPORAL PROCESSING

By

David A. Eddins

August 1993

Chairman: David M. Green
Major Department: Psychology

Estimates of auditory temporal acuity and across-frequency temporal processing were based upon psychophysical measurements of amplitude modulation detection and masked pure-tone thresholds. The first set of experiments measured the sensitivity to modulation of narrowband noise stimuli as a function of modulation frequency. Resulting temporal modulation transfer functions (TMTFs) were used to characterize the temporal response of the auditory system. TMTFs obtained for four bandwidths at three different frequency regions revealed that temporal acuity was constant across stimulus frequency region and inversely related to stimulus bandwidth.

TMTFs were independent of stimulus level for narrowband and wideband noise stimuli over a range of 50 dB. At sensation levels < 20 dB, sensitivity to modulation was

reduced. Temporal acuity estimates, however, were constant over a 70-dB range.

Temporal acuity estimates based on low-frequency stimuli may actually reflect high-frequency auditory stimulation. By restricting the region of stimulation using notched-noise masking, TMTFs revealed that similar estimates of temporal acuity for low- and high-frequency stimuliwere not due to only high-frequency stimulation. Psychometric functions for modulation detection were steeper with increasing modulation frequency (4 to 250 Hz) and were independent of stimulus bandwidth and frequency region.

Modulation masking period patterns (masked pure-tone threshold for unmodulated minus amplitude modulated noise as a function of modulation frequency) yielded another temporal acuity measure. Derived TMTFs for four signal frequency and four masker bandwidth conditions indicated essentially the same temporal acuity across signal frequency for narrowband maskers and better temporal acuity at high signal frequencies for wideband maskers.

The ability to combine temporal information across different spectral regions was investigated using a comodulation masking release (CMR) paradigm based upon pure-tone thresholds masked by narrowband stimuli having either incoherent or coherent envelopes across frequency. The influence of envelope fluctuation rate upon CMR magnitude was investigated by varying narrowband noise bandwidth and the amplitude modulation (AM) rate of tonal maskers. As

the envelope rate increased, CMR decreased. When fast (noise) and slow (AM) envelope rates were combined simultaneously, CMR values were 5 dB for coherent noise, 18 dB for coherent AM, and 23 dB for coherence at both envelope rates.

CHAPTER 1
INTRODUCTION

Understanding the dynamic properties of the auditory system is of fundamental importance to the study of hearing. Most sounds in the environment change over time. For many of these sounds, vocal communication for example, important meaning is conveyed by these temporal changes. As time, frequency, and amplitude are the principal properties of sound, any theory of audition must take into account the relations among these properties. The present studies focus on auditory temporal processing.

Temporal processing encompasses several different aspects of audition including temporal acuity, temporal summation, and spectro-temporal analysis. The studies of temporal acuity and temporal summation have a long history and a great deal is known about these dynamic processes, whereas interests in spectro-temporal processing have become widespread only recently. Temporal acuity refers to the ability of the auditory system to resolve rapid changes in time. As such, the focus of acuity research has been to estimate a minimum time constant of the auditory system. A typical estimate of temporal acuity, based on several different psychophysical paradigms, is about 2 to 3 ms (e.g. Plomp, 1964).

Temporal summation, as the term suggests, is the process of adding auditory information over time in order to facilitate signal detection or discrimination. It seems logical that, within certain limits, a longer stimulus will be easier to detect than a very brief stimulus. Temporal summation, or temporal integration, is typically measured as the stimulus level at threshold as a function of stimulus duration, and is expressed as a time-intensity trade. Signal detection improves with increasing duration up to about 200 ms, beyond which detection is relatively constant with further increases in duration. Thus, estimates of the maximum integration time are typically around 200 ms (Zwislocki, 1960).

Finally, spectro-temporal processing refers to a simultaneous comparison of temporal patterns across disparate spectral locations. Traditional theories of auditory frequency analysis (e.g. Fletcher, 1940) hold that signal detection is primarily determined by the energy within a narrow spectral region surrounding the signal, or a critical band, and that energy remote from the signal has little influence on detection. More recent studies, however, have shown that energy spectrally remote from the signal may have a dramatic influence on detectability. One manifestation of such processing is comodulation masking release, or CMR. CMR refers to the **improvement** in masked signal detection with the addition of masking energy remote from the signal frequency, provided that the additional energy has a

similar temporal pattern to the masking energy near the signal (Hall, Haggard, & Fernandes, 1984).

One goal of the present research was to estimate temporal acuity for stimuli having different spectral content. Previous studies of temporal acuity have failed to determine whether temporal acuity depends upon the frequency of the acoustic stimulus. While several investigations have indicated no effect of stimulus frequency (Green, 1973b; Shailer & Moore, 1987; Green & Forrest, 1989; Eddins, Hall, & Grose, 1992), others have implied strong effects of stimulus frequency, with temporal acuity being better at high- than low-stimulus frequencies (Buus & Florentine, 1985; Shailer & Moore, 1985; Formby & Muir, 1988). Those indicating differences in temporal acuity with frequency, however, have typically employed narrowband noise stimuli, and have often confounded noise bandwidth with changes in stimulus frequency by using bandwidths of constant proportion to the stimulus frequency.

The experiments presented in Chapters 2 and 3 were designed to specifically address the influence of stimulus frequency and noise bandwidth on estimates of temporal acuity. In Chapter 2, several experiments based upon the detection of amplitude modulation of a noise stimulus are reported. Briefly, the ability to follow the sinusoidal amplitude fluctuations of a modulated stimulus is dependent upon the temporal acuity of auditory system. By measuring the sensitivity to modulation as a function of modulation

frequency, a temporal modulation transfer function (TMTF) may be mapped. In theory, if the auditory system were linear, the TMTF would completely describe the temporal response of the system. From the TMTF, a single estimate of temporal acuity may be obtained. For broadband noise, a typical estimate of temporal acuity based on the TMTF is 2-3 ms (Viemeister, 1979). Four modulation detection experiments are presented that were designed to estimate temporal acuity for narrowband noise using the TMTF technique. TMTFs were obtained for different stimulus frequency regions, bandwidths, levels, and with notched-noise masking to restrict the region of excitation by the stimulus.

In Chapter 3, an indirect method of obtaining a TMTF, the modified masking period pattern, was used to estimate temporal acuity as a function of stimulus frequency and bandwidth. In this paradigm, the threshold for a pure-tone signal masked by either unmodulated or amplitude modulated noise is measured. The difference between thresholds in those two masker types, as a function of modulation frequency, was used to derive a TMTF, and thus to describe the temporal response of the auditory system.

A second goal of the present research was to investigate certain temporal factors that contribute to the spectro-temporal processes involved in comodulation masking release. The first experiment investigated the influence of envelope fluctuation rate upon the magnitude of CMR. This was tested in two ways. The first involved

systematically changing the bandwidth of multiple narrow-band maskers. As noise bandwidth is directly related to the rate of envelope fluctuation, this method was effective in assessing a range of envelope rates. In the second method, the rate of amplitude modulation of tonal maskers was systematically varied. Based upon previous investigations (Buus, 1985; Hall, 1986; Schooneveldt & Moore, 1987), it was expected that CMR would increase with decreasing fluctuation rate (e.g. narrower bandwidths and lower modulation frequencies). The present experiment provided a direct comparison of the two methods of envelope rate variation. The second and third experiments in Chapter 4 involved a combination of two rates of envelope fluctuation simultaneously. The primary purpose of these experiments was to determine whether CMR was a result of only the slowest envelope rate, or whether the auditory system could make comparisons of the two envelope rates separately.

CHAPTER 2

AMPLITUDE MODULATION DETECTION OF NARROWBAND NOISE: EFFECTS OF ABSOLUTE BANDWIDTH, FREQUENCY REGION, AND LEVEL

Introduction

There are two common methods used to estimate auditory temporal acuity. One method, temporal gap detection, evaluates the shortest detectable silent interval in an otherwise continuous stimulus (e.g. Plomp, 1964). A second method, amplitude modulation detection, assesses the ability to hear the sinusoidal amplitude modulation of a continuous sound. By measuring the sensitivity to modulation as a function of modulation frequency, a temporal modulation transfer function (TMTF) may be obtained (Viemeister, 1979). Often the temporal response of the auditory system is modeled as an exponential decay process or a simple low-pass filter. The utility of the modulation detection technique is clearly evident when considered in terms of such a model. When the frequency of modulation is much less than the passband of the low-pass filter, the input modulation depth will nearly equal the output modulation depth. If, however, the modulation frequency well exceeds the bandwidth of the low-pass filter, then the output of the filter will be severely attenuated compared to the amplitude of the input. By measuring modulation

detection as a function of modulation frequency, the frequency response of the low-pass filter may be mapped.

In theory, if the auditory system were linear, the TMTF would characterize the temporal response of the system to any input. Although the auditory system not strictly linear, the modulation detection approach has achieved considerable success. Excellent reviews of the TMTF and the systems analysis approach in vision and audition are provided by Cornsweet (1970) and Viemeister (1979), respectively.

One motivation for the present study was to probe the compatibility between results based upon modulation and gap detection. This study builds upon the previous gap detection study of Eddins et al. (1992). That investigation addressed the influence of stimulus bandwidth and frequency region on gap detection. It demonstrated that gap detection for a noise stimulus was highly dependent on absolute noise bandwidth, and was invariant with changes in frequency region when absolute bandwidth was held constant.

The dependence of modulation detection upon bandwidth and frequency region is not known, as these parameters often have been confounded. For example, Viemeister (1979) derived modulation transfer functions for band-limited noise stimuli centered at 200, 1000, and 10,000 Hz with bandwidths of 120, 500, and 4400 Hz, respectively. Although the time constants derived from the modulation transfer functions decreased with increasing frequency

region, the associated increase in stimulus bandwidth precluded a separation of bandwidth and frequency effects. Likewise, Formby and Muir (1988) reported shorter time constants for higher frequency stimuli, however, as the authors noted, bandwidth may have been a confounding factor (see Eddins et al. (1992) for discussion).

Perhaps the most detailed investigation of the influence of stimulus bandwidth and frequency region on modulation detection with narrowband noise was conducted by van Zanten (1980). van Zanten reported improved sensitivity to modulation with increasing stimulus bandwidth from 400 to 1600 Hz. He also reported improved sensitivity to modulation with increasing frequency region from 500 to 4000 Hz for equivalent nominal bandwidths. Comparisons across frequency region, however, may have been confounded by changes in the "effective" stimulus bandwidth due to analog filtering. The attenuation rates of the filter were 96 dB/octave. van Zanten adjusted the filter for each frequency condition to have equal bandwidth when measured at the -3 dB point. Further down on the attenuation skirts the bandwidths were not equal across frequency. One hypothesis is that the reported frequency effect resulted from an increase in the "effective" bandwidth with increasing frequency.

The confounding of frequency region with bandwidth occurs in the gap-detection literature as well. When these param

bandwidth dominates performance and frequency region has little effect (Grose, Eddins, & Hall, 1989; Eddins et al., 1992). The purpose of the first experiment of the present study was to investigate temporal acuity using a temporal modulation transfer function technique, independently varying stimulus bandwidth and stimulus frequency region to determine the influence of these parameters on modulation detection. The primary difference between this and previous investigations is the comparison of equivalent bandwidths across frequency region by rectangular windowing in the frequency domain rather than analog filtering.

In a second experiment, the influence of stimulus level on modulation detection was measured for wideband and narrowband noise. The third experiment investigated modulation detection for narrowband stimuli in the presence of a notched-noise masker. Previous investigators have suggested that estimates of temporal acuity from low-frequency noise stimuli may actually reflect high-frequency auditory processing due to the spread of excitation along the cochlea. The notched-noise masker served to restrict this spread. Psychometric functions also were measured for amplitude-modulation detection under several bandwidth and carrier frequency conditions.

Experiment 1. Effects of Bandwidth and Frequency Region

Amplitude-modulation thresholds were estimated by determining the modulation depth necessary to discriminate a noise that was sinusoidally amplitude modulated from an unmodulated noise. Modulation thresholds were measured for several modulation frequencies over a range of stimulus bandwidths at a low- (600 Hz), a mid- (2200 Hz), and a high-frequency (4400 Hz) region. Modulation transfer functions were then derived by plotting the threshold sensitivity to modulation versus modulation frequency.

Method

Subjects

Three subjects with normal hearing sensitivity (250 to 8000 Hz) participated in both experiments. Subjects ranged in age from 20 to 26 years. Each subject received extensive preliminary training in modulation detection using both wideband and narrowband carrier stimuli. Subjects were paid an hourly wage and received a 20 percent bonus upon completion of the study.

Stimuli

Three sets of band-limited stimuli were employed. The high-frequency cutoff was fixed at 600, 2200, or 4400 Hz. Four bandwidths, 200, 400, 800, and 1600 Hz, were used at the higher frequency regions. Only the 200- and 400-Hz bandwidths could be tested for the 600-Hz upper cutoff.

Two additional stimulus conditions were included to determine asymptotic bandwidth performance. The first of these was a 2000-Hz narrowband noise with an upper cutoff of 2200 Hz. The second was a broadband noise low-pass filtered at 5000 Hz. In all conditions, modulation frequencies were 4, 8, 16, 32, 64, 125, 250, and 500 Hz with the stipulation that modulation frequency did not exceed one-half the stimulus bandwidth. For example, for a bandwidth of 200 Hz, the highest modulation frequency was 64 Hz. The total signal duration was 410 ms and the entire signal was shaped by multiplying the waveforms with a $\cos^2$ function giving rise/fall times of 10 ms.

The method of generating modulated stimuli in the present experiment required the careful consideration of possible cues for discrimination that do not reflect the detection of temporal changes in a waveform. These are spectral and absolute level cues. First, consider possible spectral cues. In a simple case, a sine wave, f_c, that is amplitude modulated by a second sine wave, f_m, has three components, the carrier frequency, f_c, and two side bands with frequencies of $f_c + f_m$ and $f_c - f_m$. Similarly, an amplitude-modulated noise has sidebands that extend $\pm f_m$ from the edges of the passband. In this case, it is possible that the detection of modulation may be based on the identification of spectral changes in the signal interval, rather than temporal changes in the modulated waveform. These spectral cues would be dependent on frequency region,

owing to the relation of frequency difference limens and center frequency (Wier, Jesteadt, & Green, 1977). One way to avoid these spectral cues would be to amplitude modulate wideband noise before bandpass filtering. Thus, the bandwidth of the narrowband stimuli would be the same regardless of the presence or absence of modulation. The technique of introducing modulation prior to filtering was used by Viemeister (1979) to measure modulation detection for narrowband stimuli. In a similar fashion, several gap-detection studies have employed stimuli that were filtered after the introduction of a temporal gap in order to restrict spectral splatter (Grose et al., 1989; Eddins et al., 1992).

By filtering after amplitude modulation, the sidebands introduced by modulation are effectively reduced. To determine the effect of filtering after the modulation process, a series of computer simulations evaluated the change in modulation depth as a function of filter condition.[1] Filtering after modulation will reduce the effective modulation, partially filling in the "valleys" of the waveform. The simulations revealed that modulation depth was relatively unaffected for the filter conditions used in these experiments. Thus spectral cues were not available and the task was purely temporal in nature.

A second issue to be addressed when generating amplitude-modulated narrowband stimuli is the absolute level of the unmodulated and modulated signals. The average power

of a modulated signal is greater by $1 + m^2/2$ than the average power in the same signal when it is unmodulated. Therefore, for large depths of modulation, detection could be based on intensity level rather than the presence or absence of modulation. To counter confounding level cues, two safeguards were introduced. First, the digital waveforms were adjusted to have equal power in each interval of the forced-choice trial. To further discourage the use of a level cue, the overall noise level was varied randomly over a 10 dB range (50 ±5 dB) on each stimulus presentation.

All stimuli were digitally generated using an array processor (TDT QAP1) and 16 bit D/A converter (TDT QDA1) with a sampling period of 50 μs (20,000 Hz). For each stimulus interval, broadband Gaussian noise was generated by filling a 8192 point buffer with numbers having a Gaussian distribution and zero mean. For modulated stimuli, the broadband noise was multiplied by the function

$$m(t) = [1 + m (\sin 2\pi Ft)] \qquad \text{Eq. 2-1}$$

where m is modulation depth, $0<m<1$, and F is modulation frequency. The broadband stimuli, either modulated or unmodulated, then were digitally filtered by setting the magnitude of the Fourier coefficient to zero outside the desired pass band, and signals were adjusted to have equal power. Stimuli were presented monaurally via a Sennheiser (HD 450-13) earphone at a median spectrum level of 50 dB SPL. Output waveforms were low-pass filtered at 6000 Hz.

After low-pass filtering, image frequencies remained more than 40 dB down from the stimulus band. To mask these components, a broadband (6000 Hz low-pass) analog noise was presented continuously at a 20 dB spectrum level.

Procedure

An adaptive two-interval, two alternative forced-choice method with a three-down one-up tracking strategy was used to estimate 79.4% correct detection (Levitt, 1971). During a threshold run, modulation depth, 20 log(1/m), was titrated using an initial step size of 5 dB, which was reduced to 2 dB after the first three reversals. Threshold was estimated by averaging the modulation depth on each trial after the first four reversals. Six 70-trial blocks were used to estimate the threshold for each experimental condition. The standard error computed over six blocks was about 0.7 dB and was consistent across subjects and conditions. Each interval of the forced-choice trial was marked by a 400-ms light and visual feedback was provided after each trial. Testing was conducted in a sound-attenuating chamber and stimulus timing and response collection were controlled by a microcomputer.

Results

Modulation thresholds for several stimulus conditions are plotted in Fig. 2-1 with sensitivity to modulation,

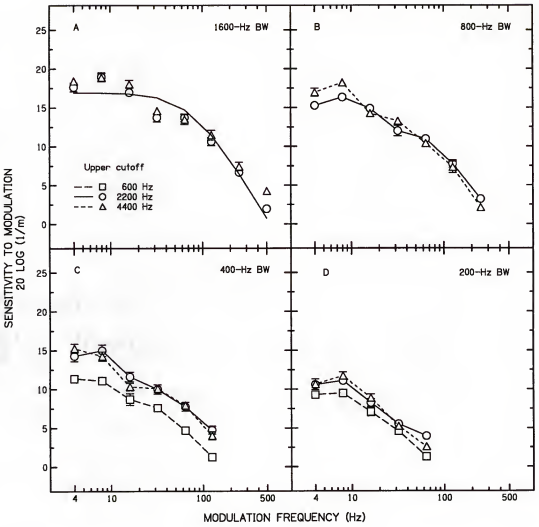

Figure 2-1. Sensitivity to modulation (mean for three listener) as a function of modulation frequency with upper cutoff frequency as the parameter. Error bars indicate standard error of the mean. Each panel represents the identified bandwidth conditions. The solid line in panel A is the fitted function to the 2200-Hz upper cutoff data, as discussed in the text.

expressed as 20 log(1/m), on the ordinate, and modulation frequency (Hz) on the abscissa. Upper-cutoff frequencies are indicated by the symbols. Each of the four panels represents a separate bandwidth condition from 1600 to 200 Hz. The solid line in panel A shows a fitted function for one stimulus condition and will be discussed later. These modulation transfer functions reflect the greatest sensitivity to modulation at very low modulation frequencies (≤8 Hz). For higher modulation frequencies, sensitivity to modulation decreases monotonically at a rate of about 3 dB/octave. The transfer functions reflect a low-pass characteristic that is similar to data from previous investigations of modulation detection (Rodenburg, 1977; Viemeister, 1977, 1979; Forrest & Green, 1987; Formby & Muir, 1988).

The data for the 2200- and 4400-Hz frequency regions are virtually superimposed for each of the four bandwidth conditions. Note that the sensitivity for the 400- and 200-Hz bandwidth conditions at the 600 Hz cutoff frequency (squares, panels C and D) is about 3 dB lower than the sensitivity for corresponding bandwidths at 2200 and 4400 Hz. This decrease in sensitivity is relatively constant across all modulation frequencies. Therefore transfer functions for the three cutoff frequencies are similar in form.

Figure 2-1 reveals that increasing stimulus bandwidth results in a corresponding increase in sensitivity to

modulation. This systematic increase is true for each of the three cutoff frequency conditions tested. Across the different bandwidth conditions, asymptotic performance for low modulation frequencies was about 10 dB (200 Hz), 14 dB (400 Hz), 17 dB (800 Hz), and 19 dB (1600 Hz). Thus the improvement in sensitivity was about 3 dB/octave of bandwidth up to a bandwidth of 1600 Hz. Beyond a bandwidth of 1600 Hz, sensitivity to modulation continued to improve. Thresholds for low modulation frequencies were about 19 dB and 23 dB for the 2000-Hz bandwidth and 5000-Hz low-pass conditions, respectively.

Since the form of the modulation transfer function resembled that of a simple low-pass filter, the data were fit with the transfer function for a simple low-pass filter of the form

$$10\log\left(1/(1+(\alpha F)^2)\right) \qquad \text{Eq. 2-2}$$

From this fitted function, an associated time constant was derived where $\tau=1/(2\pi F_c)$.[2] F_c was the -3 dB cutoff frequency. Low-pass functions were fitted to the modulation transfer functions for each listener and condition. The rms error for the fitted functions across listeners and conditions ranged from 0.4 to 2.6 dB. Time constants and corresponding -3 dB bandwidths for each of the fitted functions are presented in Table 2-1. A sample fitted function is shown in panel A, Fig. 2-1 for the 2200-Hz cutoff frequency (solid line).

TABLE 2-1. Values of τ and -3 dB bandwidths associated with fitted low-pass functions for each stimulus condition and subject.

Bandwidth		Upper frequency cutoff					
		600 Hz		2200 Hz		4400 Hz	
		-3 dB BW	τ	-3 dB BW	τ	-3 dB BW	τ
200 Hz	S1	34.0	4.7	28.6	5.6	32.2	4.9
	S2	25.0	6.4	38.6	4.1	16.7	9.5
	S3	20.8	7.6	24.1	6.6	22.1	7.2
	MEAN	26.6	6.2	30.4	5.4	23.7	7.2
400 Hz	S1	48.3	3.3	41.6	3.8	53.8	3.0
	S2	35.4	4.5	39.8	4.0	28.3	5.6
	S3	46.6	3.4	40.6	3.9	41.9	3.8
	MEAN	43.4	3.7	40.6	3.9	41.3	4.1
800 Hz	S1			60.7	2.6	53.0	3.0
	S2			59.6	3.7	47.0	3.4
	S3			59.9	2.7	34.3	4.7
	MEAN			60.1	3.0	44.7	3.7
1600 Hz	S1			70.4	2.3	90.3	1.8
	S2			76.1	2.1	94.1	1.7
	S3			91.1	1.8	75.8	2.1
	MEAN			79.2	2.0	86.7	1.8
2000 Hz	S1			78.3	2.0		
	S2			70.4	2.3		
	S3			74.6	2.1		
	MEAN			74.4	2.1		
LOW-PASS	S1			73.7	2.2		
	S2			77.3	2.1		
	S3			71.2	2.2		
	MEAN			74.1	2.2		

Two-way repeated measures analyses of variance on the time constants indicated no statistically significant effect of changing frequency region for the 200- and 400-Hz bandwidths at three cutoff frequencies ($F_{2,12}=0.82$, $p<0.01$). Further, no significant frequency effects were noted for the four bandwidths at the two higher cutoff frequencies ($F_{1,16}=2.6$, $p<0.01$). The effect of noise bandwidth was statistically significant, where τ decreased as bandwidth increased. Repeated measures ANOVAs indicated significantly different τ values both for the 200- and 400-Hz bandwidths at three cutoff frequencies ($F_{1,12}=13.47$, $p<0.005$) and for the four bandwidths at the two higher cutoff frequencies ($F_{3,16}=17.26$, $p<0.005$). Thus τ was inversely related to stimulus bandwidth for bandwidths $\leq$1600 Hz. For bandwidths $\geq$1600 Hz, τ was relatively constant, as shown in Table 2-1. Estimates of τ were relatively invariant in terms of stimulus cutoff frequency.

Because the time constants did not differ across frequency region, they were averaged across frequency region and plotted against stimulus bandwidth as shown in Fig. 2-2 (squares). On the same graph is shown the average gap-detection data from Eddins et al. (1992). Both modulation and gap detection data reflect a decrease proportional to the square root of the change in bandwidth for bandwidths $\leq$1600 Hz, as indicated by the fitted lines (see also Grose et al., 1989). Although the absolute τ values for modulation detection are shorter (by a factor of 3.1) than

the gap thresholds reported by Eddins et al., the form of the functions is remarkably similar. This absolute difference is not surprising as τ values for modulation detection are derived time constants, whereas the gap detection data are empirical thresholds.

Discussion

Two primary results emerge from the data. First, the time constants associated with modulation transfer functions derived for narrowband noise stimuli do not vary with changing frequency region. This result is in agreement with recent gap detection experiments (Eddins et al., 1992; Grose et al., 1989) and is consistent with many previous accounts of modulation and gap detection with narrowband noise when those data are considered in terms of stimulus bandwidth rather than center frequency (Viemeister, 1979; Fitzgibbons & Wightman, 1982; Fitzgibbons, 1983, 1984; Shailer & Moore, 1983, 1985; Buus & Florentine, 1985; Glasberg, Moore, & Bacon, 1987; Moore & Glasberg, 1988; Formby & Muir, 1988). Second, the time constants associated with modulation transfer functions decrease monotonically with increasing stimulus bandwidth for bandwidths $\leq$1600 Hz. Values of τ become asymptotic for bandwidths wider than 1600 Hz.

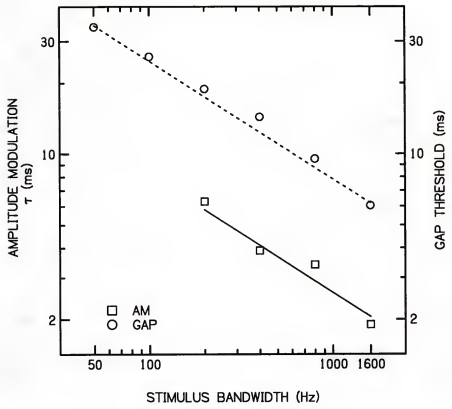

Figure 2-2. Temporal acuity as a function of stimulus bandwidth. Modulation data (squares) and gap detection data (circles) from Eddins et al. (1992). Fitted lines indicate improvement proportional to the square root of the change in stimulus bandwidth.

The modulation transfer functions reported here are consistent with previous modulation detection data both in terms of bandwidth dependence and absolute value. The sensitivity to modulation improved with increasing stimulus bandwidth for bandwidths from 200 to ≥2000 Hz. Likewise, Formby and Muir (1988) reported increasing sensitivity to modulation for bandwidths up to and beyond 4000 Hz. Several other investigators have demonstrated systematic improvements in sensitivity to modulation with increasing noise bandwidth (Rodenburg, 1977; Viemeister, 1979; van Zanten, 1980; Bacon & Viemeister, 1985; Formby & Muir, 1988). The absolute sensitivity to modulation reported here is consistent with previous reports as well. When making comparisons among studies, however, it is important to recognize differences in stimulus duration, stimulus bandwidth, the method of filtering, and the obtained percent correct, as each of these parameters influence detection.

Note that the sensitivity to modulation at the 4-Hz modulation frequency is slightly reduced (1 to 2 dB) relative to 8 Hz. Similar results have been reported previously when gated carriers were employed (Viemeister, 1979). Such a decrease, however, does not occur when continuous carriers are used. As suggested by Viemeister, the reduced sensitivity may be explained by a reduced number of "looks" at the cycle of modulation. In the present experiment, the duration of the carrier was 410 ms,

providing 3.2 cycles of modulation at 8 Hz and only 1.6 cycles of modulation at 4 Hz. This line of reasoning suggests that 1.6 cycles of modulation are insufficient to produce maximal performance. It is somewhat surprising that performance is dependent upon durations several orders of magnitude greater than the typical time constant of the TMTF. Nonetheless, data reported by Viemeister and data collected in this laboratory indicated an interaction between stimulus duration and modulation frequency such that a fixed number of modulation cycles produces roughly constant detectability at very low modulation frequencies (2-8 Hz). It remains unclear why such effects are not found for continuous carriers. Viemeister proposes an explanation based upon a slow adaptation process of several hundred milliseconds that occurs at the onset of a gated carrier and effectively masks the first few cycles of modulation. The interested reader is referred to Viemeister (1979) for a more detailed discussion.

The present data are in good agreement with a number of other studies indicating that temporal acuity is independent of frequency region. These studies include investigations of gap detection with single sinusoids, the detection of a sinusoid embedded in a temporal gap in noise, the discrimination of Huffman sequences, and temporal order detection (Green, 1973; Shailer & Moore, 1987; Moore & Glasberg, 1988; Moore, Glasberg, Plack, & Biswas, 1989; Green & Forrest, 1989; Plack & Moore, 1990).

In contrast to the studies considered above, two studies have indicated that modulation detection is frequency dependent (van Zanten, 1980; Formby & Muir, 1988). Stimulus bandwidth, however, may have been a confounding factor in both of these studies. First, Formby and Muir (1988) compared a high-frequency (4000-6500 Hz) and a low-frequency (4000-Hz low-pass) condition, and reported both shorter τ values for modulation detection and shorter gap thresholds for their high-frequency condition. By using the earphone transfer function as the high-frequency cutoff in the high-frequency condition, the effective bandwidth may have actually been wider than the bandwidth of the low-frequency condition, leading to an apparent frequency effect. The authors recognized this limitation and subsequent informal testing by Eddins et al. (1992) using the same conditions and sharp filtering indicated longer high-frequency gap thresholds.

Second, van Zanten (1980) reported improved sensitivity to modulation with increasing frequency region for equivalent nominal bandwidths. While the conditions employed by van Zanten and those in the present study are similar, one important difference between the two studies was the filtering technique. van Zanten used analog filtering with relatively shallow filter slopes, whereas stimuli in the present study were digitally filtered by setting the magnitude of the Fourier coefficient to zero outside the desired pass band. Using the latter technique,

the filter slopes were extremely steep and therefore the "effective" bandwidths were equal across frequency region. However, analog filtering results in very different "effective" bandwidths across frequency. For example, two Krohn-Hite 3342 analog filters connected in series, as in the van Zanten study, yield a nominal attenuation rate of 96 dB/octave. Thus a stimulus with a nominal 400-Hz bandwidth centered at 500 Hz has a -10 dB bandwidth of 465 Hz and a -20 dB bandwidth of 560 Hz. In contrast, a 400-Hz bandwidth centered at 4000 Hz has a -10 dB bandwidth of 1280 Hz and a -20 dB bandwidth of 2010 Hz. Thus, the differences in modulation threshold across frequency region reported by van Zanten may reflect an increase in "effective" signal bandwidth as a consequence of analog filtering rather than a true frequency effect. Such an argument is supported by the dependence of modulation threshold on stimulus bandwidth.

To test this hypothesis, modulation thresholds were measured using both analog filtering and digital filtering, as in the present study. A description of this experiment and the results are presented in the Appendix. Given a nominal bandwidth of 800 Hz, the digital filtering technique resulted in similar modulation-detection thresholds at cutoff frequencies of 2200 and 4400 Hz. However, analog filtering yielded better sensitivity to modulation (about 3 dB) at 4400 Hz than 2200 Hz. The difference in filtering techniques appears to account for differences in

sensitivity to modulation reported here and by van Zanten and supports the hypothesis that modulation detection is influenced by stimulus bandwidth rather than frequency region.

One issue addressed in earlier studies of temporal acuity is the possible influence of peripheral filtering on measures of temporal acuity. At center frequencies of 2000 and 4200 Hz, estimated equivalent rectangular bandwidths (ERBs) are about 240 Hz and 530 Hz, respectively (Glasberg & Moore, 1990). Therefore, it might be expected that modulation thresholds for certain conditions would differ across these two frequency regions as a result of peripheral filtering. The 400-Hz bandwidth conditions used in the present study allow a comparison across sub-critical (4400-Hz condition) and supra-critical (2200-Hz condition) band stimuli at these center frequencies. For the 400-Hz bandwidth, modulation transfer functions at 2200 and 4400 Hz did not differ. Further, for a stimulus bandwidth clearly wider than an ERB at the 2200 and 4400 Hz regions (e.g., the 1600-Hz bandwidth condition), modulation detection did not differ. Thus the influence of peripheral filtering is not readily apparent in the present modulation detection data. A similar result was obtained by Eddins et al. (1992) for gap detection.

Comparable detection results for low- and high-cutoff frequencies might be explained by a linear combination of the outputs of several critical bands. Such an explanation

has been suggested to account for bandwidth effects reported for intensity discrimination of noise stimuli, the detection of temporal gaps, and modulation detection (Green, 1960; De Boer, 1966; Schacknow & Raab, 1976; Viemeister, 1979; Shailer & Moore, 1983; 1985; Bacon & Viemeister, 1985; Formby & Muir, 1988; Grose et al., 1989; Eddins et al., 1992;). A recent report by Formby, Forrest, and Raney (1992) indicated that the empirical results of Formby and Muir (1988) could be accurately modeled by a single-channel envelope detector. Their use of a pre-detection filter approximately the width of one critical band suggests a strong dependence of modulation detection on peripheral auditory filtering. It is difficult to reconcile these inconsistencies without additional modeling.

Although the modulation and gap detection data of Fig. 2-2 are proportional to each other across frequency region and stimulus bandwidth, two inconsistencies remain. First, whereas sensitivity to modulation was poorer at the 600-Hz cutoff frequency than at either 2200 or 4400 Hz, gap detection thresholds were similar across the 600-, 2200-, and 4400-Hz cutoff frequencies. Reasons for this difference in sensitivity at the 600-Hz upper cutoff are unclear. Second, estimated τ values for modulation detection decreased as bandwidth increased up to 1600 Hz. This improvement parallels the improvement reported for gap-detection thresholds over the same bandwidth range. For bandwidths wider than 1600 Hz, τ values were relatively constant at

about 2 ms. The sensitivity to modulation, however, continued to increase for bandwidths >1600 Hz. It is expected that gap-detection thresholds would also continue to improve for bandwidths wider than 1600 Hz, reaching a minimum value of 2-3 ms, as typically reported. The present results indicate that τ and gap-threshold are closely related for bandwidths less than 1600 Hz. It is possible that for wider bandwidths, gap-detection thresholds are more closely related to the sensitivity to modulation than to estimated τ values. Formby and Muir (1988) reported such a relation for bandwidths ≥2000 Hz.

Experiment 2: Effects of Stimulus Level

Both the form of the modulation transfer function and the sensitivity to modulation as measured with broadband noise appear to be largely independent of stimulus level over the range of spectrum levels from 20 to 50 dB (Viemeister, 1979). A question of interest to the present study is whether this level independence holds for narrowband stimuli. In this experiment, modulation detection was measured as a function of level for both wideband and narrowband noise carriers. Knowledge of the influence of stimulus level on modulation detection for narrowband carriers aided in determining the level of notched-noise maskers to be employed in a subsequent experiment.

Method

Subjects

Three new subjects with normal hearing sensitivity (250 to 8000 Hz) participated in this experiment. Subjects ranged in age from 20 to 31 years. Each subject received several hours of training in modulation detection using wideband and narrowband noise carriers prior to data collection. Subjects were paid an hourly wage and received a 20 percent bonus upon completion of the study.

Stimuli

Stimulus generation was identical to the previous experiment. Modulation detection was measured for a wideband noise (0 to 6000 Hz) and two narrowband noises: a 400-Hz bandwidth with an upper cutoff of either 600 or 2200 Hz. The frequency of modulation was either 4, 8, 16, 32, 64, or 125 Hz for the narrow bandwidths. Additional modulation frequencies of 250 and 500 Hz were included for the wideband noise. Stimuli were presented at the following spectrum levels: 50, 30, 10, and -10 dB. In two cases, a level of -20 dB was also included.

The modulation detection procedure was identical to that of Exp. 1.

Results and Discussion

Figure 2-3 shows sensitivity to modulation, expressed as 20 log(1/m), as a function of modulation frequency for the three conditions. The spectrum level of the stimulus

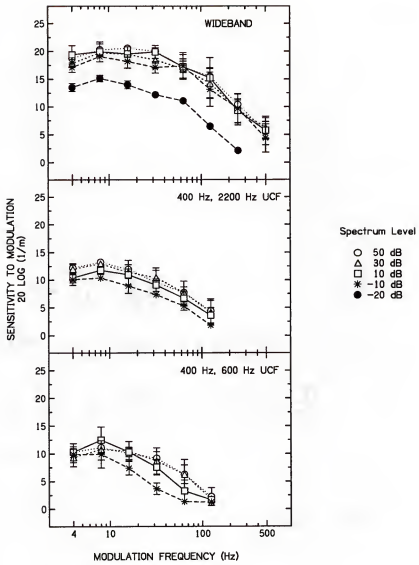

Figure 2-3. Sensitivity to modulation (mean for three listeners) as a function of modulation frequency with noise spectrum level as the parameter. The upper panel is for a wideband (0 to 6000 Hz) masker. The middle and lower panels show data for a 400-Hz bandwidth at upper cutoffs of 2200 and 600 Hz, respectively. Error bars indicate standard error of the mean.

is the parameter, as denoted by the symbols. The form of the modulation transfer functions were consistent with those in Fig. 2-2. The sensitivity to modulation was greatest at low modulation frequencies and decreased about 3 dB/octave for higher modulation frequencies. For the wideband condition (upper panel), modulation transfer functions were virtually superimposed over the range from -10 to 50 dB. At the lowest level tested, -20 dB, the entire modulation transfer function was displaced vertically indicating a decrease in sensitivity to modulation at all modulation frequencies. The form of the function at -20 dB was similar to those for higher levels, suggesting little change in the estimated time constants.

The middle panel of Fig. 2-3 shows data for a 400-Hz bandwidth with an upper cutoff of 2200 Hz. Sensitivity to modulation is somewhat reduced for the lowest level tested (-10 dB), as shown by the asterisks. Again the modulation transfer functions generally demonstrate the same form across the four spectrum levels, indicating similar time constants for the different levels.

Finally, the lower panel of Fig. 2-3 shows sensitivity to modulation for a 400-Hz bandwidth with an upper cutoff of 600 Hz. The data for the three highest levels show considerable overlap, while data for the lowest level (asterisks) falls slightly below the rest.

A repeated measures analysis of variance comparing sensitivity to modulation for the different stimulus levels

was performed for each of the three bandwidth conditions. A summary of the main effects and interactions is presented in Table 2-2. As expected, for all three conditions, the effect of changing modulation frequency was significant, with sensitivity to modulation decreasing as modulation frequency increased. Furthermore, the effect of level was also significant at each stimulus condition. There were no interactions between stimulus level and modulation frequency, confirming previous observations that the form of the functions did not differ across the levels. The effects of stimulus level were dominated by the lowest test level where sensitivity was significantly reduced for each bandwidth condition.

For each of the three stimulus conditions, the absolute threshold for the unmodulated carrier was measured. The results were consistent across the three listeners. Average absolute thresholds in dB spectrum level were -29.8 for the wideband condition, -26.5 for the 400-Hz bandwidth, 2200-Hz upper cutoff, and -15.0 for 400-Hz bandwidth, 600-Hz upper cutoff. Thus, at the lowest spectral levels tested, the sensation level was about 10 dB for the wideband condition, 15 dB for the 2200-Hz condition, and 5 dB for the 600-Hz condition. Though not dramatically different, it is possible that the form of the modulation transfer function for the 600-Hz condition at the -10 dB level was influenced by the relatively low sensation level of that stimulus. Overall these results suggest that the

TABLE 2-2. The F ratios and significance levels for repeated measures analyses of variance for the three stimulus conditions of Exp. 2. The factors were noise spectrum level, modulation frequency (f_m), and level-modulation frequency interactions.

Condition	Factor	*F* ratio	Significance
400-Hz BW	Level	$F_{(3,48)} = 12.07$	$p<0.01$
600-Hz UCF	f_m	$F_{(5,48)} = 40.32$	$p<0.01$
	Level X f_m	$F_{(15,48)} = 0.89$	$p<0.05$ n.s.
400-Hz BW	Level	$F_{(3,48)} = 9.69$	$p<0.01$
2000-Hz UCF	f_m	$F_{(5,48)} = 50.78$	$p<0.01$
	Level X f_m	$F_{(15,48)} = 0.14$	$p<0.05$ n.s.
Wideband	Level	$F_{(4,80)} = 45.31$	$p<0.01$
	f_m	$F_{(7,80)} = 103.80$	$p<0.01$
	Level X f_m	$F_{(28,80)} = 0.48$	$p<0.05$ n.s.

sensitivity to modulation is fairly constant for stimuli ranging from about 20 to 70 dB sensation level. Furthermore, the effect of stimulus level is the same for narrowband stimuli (e.g. 400-Hz bandwidth) as for wideband stimuli (6000-Hz low-pass).

The results of this experiment are interesting in terms the way in which modulation depth is processed by the auditory system. The sensitivity to modulation varied little over a wide range of spectral levels (-10 to 50 dB) although the level of the noise at the minimum of a modulation cycle varied widely over that range. For example, in the wideband noise with fm = 8 Hz, the sensitivity to modulation was about 18 dB for both the -10 and the 50 dB levels. The level of the noise at the minimum of a modulation cycle was -11 dB and 49 dB for the -10 and 50 dB stimuli, respectively. Obviously that quantity is not of primary importance for modulation detection. Rather it seems that modulation detection depends upon the relative depth of modulation. This constant performance over a range of stimulus levels for a given value of 20 log(1/m) follows Weber's law, which simply states that the smallest detectable change in a stimulus is proportional to the magnitude of that stimulus. Models of temporal resolution have accounted for this Weber's-law behavior in the "decision" stage, using a quantity such as the variance of the output of the hypothetical temporal integrator or a max/min ratio of the output as the decision variable (Viemeister,

1979; Green & Forrest, 1989). The present data indicate that such Weber's-law behavior holds for narrowband stimuli as well as wideband stimuli.

Experiment 3: Effects of Notched-Noise Masking

Several investigators have suggested that estimates of temporal acuity are based upon the highest frequency channels in the auditory system excited by the stimulus (e.g. Formby & Muir, 1988). It is conceivable that the above estimates of temporal acuity for low-frequency noise bands were actually based on the excitation of high-frequency regions of the auditory system due to the spread of excitation along the cochlea. A popular method used to restrict auditory stimulation to a narrow frequency region is to employ simultaneous notched-noise masking. Thus, in the following experiment the spread of excitation from low- to high-frequency regions was limited by measuring modulation detection for a narrowband noise carrier in the presence of a simultaneous notched-noise masker whose stop band was centered on the carrier band. The noise carrier had a bandwidth of 400 Hz and upper cutoff frequencies of either 600, 2200, or 4400 Hz.

Method

Subjects

Three subjects with normal hearing sensitivity (250 to 8000 Hz) participated in this experiment. Subjects S1 and

S2 had participated in the previous experiment. Subject S3 was new to the experiment and received several hours of practice in modulation detection without masking noise prior to data collection.

Stimuli

Carrier stimuli were generated in a manner identical to that described in Exps. 1 and 2. Stimulus conditions included a 400-Hz bandwidth with upper cutoffs of 600, 2200, and 4400 Hz, and modulation frequencies of 4, 8, 16, 32, 64, and 125 Hz. Each carrier was accompanied by a notched-noise masker which was created in the following manner. First, broadband Gaussian noise was generated by filling a 16394 point buffer with numbers having a Gaussian distribution and zero mean. The spectral notch was introduced by transforming the broadband noise into the frequency domain by means of an FFT and then setting the magnitude of the Fourier coefficients to zero within the desired stop band. The center frequency of the notch was identical to the center frequency of the carrier band. A subsequent inverse FFT yielded the desired waveform.

Since auditory filtering is generally assumed to be constant relative to the frequency of stimulation, the distance between the spectral edges of the notched-noise masker and the stimulus band were chosen to be 0.02 times the center frequency of the stimulus band. Thus the notch-width was larger than the bandwidth of the stimulus band by 0.04 times the stimulus center frequency. Informal listen-

ing indicated that with equal distance between the spectral edges of the masker and stimulus bands, the 4400-Hz stimulus was less audible than the 600- or 2200-Hz stimuli. The use of a notchwidth dependent on frequency region was meant to control for changes in the audibility of the masked stimulus band with changes in center frequency. In the case of a 400-Hz band, for example, with an upper cutoff of 2200 Hz (1800 to 2200 Hz), the notch extended from 1760 Hz (1800 - 0.02·2000) to 2240 Hz (2200 + 0.02·2000), yielding a notch width of 480 Hz. Similarly, the width of the notch for the 400-Hz condition with an upper cutoff of 4400 Hz was 560 Hz.

All stimuli were shaped with a 10 ms $\cos^2$ envelope. The total masker duration was 820 ms. The total carrier duration was 410 ms and the carrier was temporally centered within the masker, leaving a 205-ms fringe preceding and succeeding the carrier. As in Exp. 1, the carrier band had a spectrum level of 50 dB. The spectrum level of the notched masker was chosen to be 40 dB based on the previous experiment which demonstrated that the form of the modulation transfer function was fairly constant for signal to masker ratios as low as -10 dB.

The procedure was identical to that of Exp. 1.

Results and Discussion

Figure 2-4 shows sensitivity to modulation as a function of modulation frequency with upper cutoff frequency as

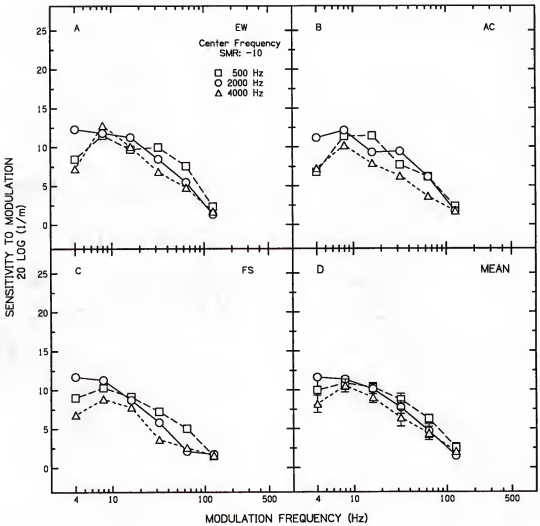

Figure 2-4. Sensitivity to modulation (mean for three listeners) as a function of modulation frequency with stimulus center frequency as the parameter. Noise carriers were 400-Hz wide and were presented with simultaneous notched-noise maskers (10 dB below the carrier level). Data in panels A to C are for individual listeners. Panel D shows the mean data where error bars indicate the standard error of the mean.

the parameter. Panels A-C show the individual data for three listeners. Error bars are the standard errors of the mean. Panel D shows the mean data across the three listeners. The form of the modulation transfer functions was similar to those reported above; the greatest sensitivity to modulation occurred at low modulation frequencies and decreased about 3 dB per octave for higher modulation frequencies. As in Fig. 2-1, the sensitivity to modulation was slightly poorer at 4 Hz than 8 Hz, by 1 to 2 dB. There was a small but systematic effect of changing frequency characterized by decreasing sensitivity to modulation from 600 to 4400 Hz. This is most clearly demonstrated in the mean data shown in panel D. These differences were apparent in a statistical analysis of the individual data as well. A repeated measures analysis of variance revealed a weak but significant main effect of frequency region ($F_{2,36}=5.09$, $P<0.05$) and a stronger main effect of modulation frequency ($F_{5,36}=45.94$, $p<0.01$). The effect of frequency region is consistent with the relatively small changes in sensitivity to modulation from 600 to 4400 Hz. The lack of an interaction between frequency region and modulation frequency is consistent with the similarity noted in the form of the modulation transfer functions across frequency regions.

The data were fit with the low-pass functions given in Eq. 2-2. Time constants then were calculated from the fitted functions for the individual and mean data of

Fig. 2-4. Fits to the mean data were representative of the individual data and the resulting time constants were 3.0, 4.1, and 2.9 ms at 600, 2200, and 4400 Hz, respectively. These time constants do not reflect a systematic change with frequency, in agreement with visual and statistical analyses which revealed differences in sensitivity to modulation but no difference in the form of the functions across frequency region.

The changes in sensitivity to modulation are somewhat different from the data of Exps. 1 and 3. In those experiments, sensitivity to modulation was 2-3 dB better at the 2200- and 4400-Hz regions than at the 600-Hz region. With notched-noise masking, the difference in sensitivity to modulation was less than a dB across frequency, and sensitivity was actually best at the lowest frequency region.

The form of the modulation transfer functions and their associated time constants are very similar across frequency region, in good agreement with our previous results. This suggests that temporal acuity is very nearly the same across different frequency regions. The fact that modulation detection is similar with and without notched-noise masking suggests that modulation detection is not simply due to the excitation of high-frequency regions.

Experiment 4: Psychometric functions

It is often convenient to know the underlying psychometric function for a particular psychophysical task.

While psychometric functions for visual modulation detection are known (Laming, 1986), psychometric functions have not been reported for the detection of amplitude modulation for audition. In the following experiment, psychometric functions were determined for amplitude-modulation detection under several stimulus conditions.

Method

Subjects

The 3 subjects from Exp. 1 participated in this experiment.

Stimuli

Stimulus generation was identical to the previous experiment. Stimulus conditions included a 1600-Hz bandwidth with an upper frequency cutoff of 2200 Hz and modulation frequencies of 4, 8, 16, 32, 64, 125, and 250 Hz. Additionally a 400-Hz bandwidth with upper cutoffs of 600, 2200, and 4400 Hz, and a 1600-Hz bandwidth with upper cutoffs of 2200 and 4400 Hz, each were evaluated for a modulation frequency of 16 Hz.

Procedure

To generate a single psychometric function, five modulation depths were estimated that would span the range of the function. These estimates were based on the modulation depth yielding 79.4% correct detection in Exp. 1. In two cases, a sixth depth was included to define better the psychometric function. As in the first experiment, a

two-interval, two-alternative forced-choice paradigm with visual feedback was employed. The standard was unmodulated noise and the signal was an amplitude-modulated noise with a modulation depth of 20 log(m). For each condition, the resulting percent correct, P(c) for six 50-trial blocks were averaged and taken as the percent correct for a particular modulation depth.

Results

Psychometric functions for three subjects and seven modulation frequencies are shown in Fig. 2-5 with percent correct versus 20 log(m). The stimulus bandwidth was 1600-Hz with an upper-cutoff frequency of 2200 Hz. Psychometric functions were consistent across subjects although there were slight differences in sensitivity. These differences were also apparent in the previous experiment. Standard error for each data point was about 2.2 percent. Psychometric functions for the 4-Hz modulation frequency were relatively shallow and spanned a range of about 14 dB. For the 250-Hz modulation frequency, the psychometric function was nearly twice as steep and represented a range of only about 8 dB. Thus, as modulation frequency increased, the range of the psychometric functions decreased.

To better quantify the psychometric functions, a least squares fitting technique was used that employed a cumulative Gaussian function of the form

$$P(c) = \Phi\ (a \cdot m^{k}) \qquad \text{Eq. 2-3}$$

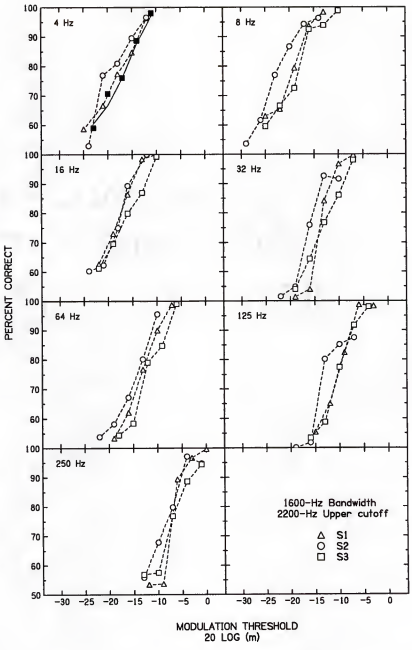

Figure 2-5. Psychometric functions, percent correct as a function of modulation threshold (dB), for three subjects. The noise stimulus had a 1600-Hz bandwidth and a 2200-Hz upper cutoff. Modulation frequency ranged from 4 to 250 Hz. The solid line in the 4-Hz panel is the fitted function for S3 as discussed in the text.

where k is the slope parameter and m is linear from 0 to 1. Values of the constant k for each stimulus condition and subject are presented in Table 2-3. The rms error ranged from about 0.3 to 5.0 percent. The solid line in upper left panel represents the fitted function for S3 in the 4-Hz condition. In general, the slope of the psychometric function increased as the modulation frequency. While slope values were non-monotonic, for each listener the value of the slope parameter, k, tended to increase with increasing modulation frequency from 4 to 250 Hz.

To test the effects of frequency region, psychometric functions were measured for a 400-Hz bandwidth at three frequency regions using a 16-Hz modulation rate. Functions were similar across subjects. The values of k are shown in Table 2-3. Slope values revealed no obvious trend across frequency region. Each function spanned a range of about 12 dB. Data for the 600-Hz region revealed reduced sensitivity to modulation as demonstrated by a shift in the psychometric function to greater modulation depths. Psychometric functions for a 1600-Hz bandwidth and a 4400-Hz cutoff frequency (16 Hz modulation rate) were virtually identical to those at 2200 Hz. A comparison of the two bandwidth conditions revealed no consistent difference in slope at 400- and 1600-Hz and increased sensitivity to modulation with increasing bandwidth.

TABLE 2-3. Values of k, the slope parameter, associated with the fitted psychometric functions.

Bandwidth				1600				
Upper cutoff				2200				
Mod. Freq.		4	8	16	32	64	125	250
	Subj.							
	S1	1.3	1.6	1.8	6.5	2.1	2.6	7.2
k	S2	1.5	1.7	2.5	2.9	1.9	2.2	2.1
	S3	1.4	1.5	1.4	1.7	1.9	2.5	1.9
	AVG	1.4	1.6	1.9	3.7	2.0	2.4	3.7

Bandwidth			400			1600	
Upper cutoff		600	2200	4400		4400	
Mod. Freq.		16	16	16		16	
	Subj.						
	S1	2.4	2.4	3.7		1.8	
k	S2	4.9	2.8	1.5		1.8	
	S3	1.7	1.5	1.5		2.0	
	AVG	3.0	2.2	2.2		1.9	

Discussion

A comparison of the psychometric functions across cutoff frequencies revealed similar slopes. Further, a difference in sensitivity to modulation at the lowest (600 Hz) frequency region was found, as in Exp. 1. For a 16-Hz modulation rate, the slopes of the psychometric functions showed little variation with increasing bandwidth, although sensitivity to modulation increased as bandwidth increased. Thus the form of the psychometric function for modulation detection in narrowband noise was not strongly dependent on frequency region nor on noise bandwidth. The most intriguing result of this experiment is the variation in slope with increasing modulation frequency. Under most circumstances, changing a parameter within a specific psychophysical task yields psychometric functions of similar slope and range of sensitivity, while shifting the function in absolute sensitivity. For modulation detection with narrowband stimuli, this is not the case. Psychometric functions tended to be steeper as modulation frequency increased.

Conclusions

Experiment 1 measured the detection of amplitude modulation in narrowband noise. The resulting modulation transfer functions exhibited the characteristic low-pass filter form. Experiment 2 investigated the influence of carrier level on modulation detection. Experiment 3

examined modulation detection in the presence of a notched-noise masker. Finally, experiment 4 measured psychometric functions for amplitude modulation detection in narrowband noise. From these experiments the following may be concluded.

1) Temporal acuity, as estimated by τ derived for temporal modulation transfer functions, varies inversely with stimulus bandwidth for bandwidths ≤1600 Hz, and remains constant for wider bandwidths.

2) Estimates of τ do not depend on the frequency location of the noise band.

3) Both of these results are consistent with estimates of temporal acuity based on gap detection in narrowband noise. Furthermore, the lack of a frequency effect is consistent with studies of sinusoidal gap detection, the detection of a sinusoid embedded in a temporal gap in noise, Huffman sequence discrimination, and temporal order detection.

4) Sensitivity to modulation is reduced at very low frequency regions as compared to mid- and high-frequency regions.

5) Absolute sensitivity to modulation increases with increasing stimulus bandwidth to bandwidths >2000 Hz.

6) Modulation detection is quite stable for changes in carrier level over the range of 10 to 50 dB spectrum level. At lower levels, the form of the TMTF is little changed, however sensitivity to modulation is reduced. These results hold for narrowband (400 Hz) as well as wideband

noise carriers and are independent of the center frequency of the carrier.

7) TMTFs measured in the presence of a notched-noise masker, designed to restrict the region of stimulation, are generally consistent with the above results. Time constants estimated from the TMTF are independent of frequency region. The results imply that TMTFs for low-frequency carriers do not simply reflect temporal process invoked by the excitation of higher frequency regions.

8) In general, psychometric functions for modulation detection in narrowband noise tend to have steeper slopes (on a 20 log(m) scale) with increasing modulation frequency from 4 to 250 Hz.

9) The slope of the psychometric function does not depend strongly on stimulus frequency region or noise bandwidth.

Notes

[1] A series of computer simulations were performed in an attempt to quantify the difference in modulation depth between stimuli that are filtered before and after amplitude modulation. The sigma-to-mean ratio of the envelope magnitude was used as the main simulation statistic. We compared this quantity before and after filtering to determine how restricting the noise bandwidth reduced the effective modulation depth. Over the range of stimulus bandwidths and frequencies employed, little change was noted in this measure.

These simulations are not completely convincing because it is unclear how one should define "effective modulation depth." Until it is understood how modulation is detected by the auditory system, there is no way of knowing the appropriate statistic to use in such simulations. In the meantime, it is doubtful that filtering after modulation had any appreciable effect on the thresholds measured in these experiments.

[2] Several fitting procedures have been used previously to obtain a summary statistic for modulation transfer functions. For example, Forrest and Green (1987) estimated a -3 dB point using a least-squares best fit line to the data for modulation frequencies ≥8 Hz. Formby and Muir (1988) used a least-squares fitting technique employing a low-pass function having a -3 dB/octave slope beyond the cutoff bandwidth. The present fitting technique employed a simple low-pass filter having -6 dB/octave slope. Although the data appear to have a slope closer to -3 dB/octave, the relatively limited range of frequencies used in modulation detection experiments restrict precise determination of attenuation characteristics. The majority of modulation frequencies used lie on the "bow" of the filter function rather than on the -6 dB/octave slope. The fitted function employed in this study provided a reasonably stable summary statistic and the fitted function corresponds to a well known physical process.

CHAPTER 3
MODIFIED MASKING PERIOD PATTERNS: INFLUENCES OF SIGNAL FREQUENCY AND MASKER BANDWIDTH

Introduction

The modified masking period pattern is an indirect method for estimating auditory temporal acuity. In this paradigm, pure-tone thresholds are measured in the presence of either an unmodulated or an amplitude modulated masking noise. The threshold difference between the unmodulated and modulated masking conditions is used to estimate the depth of modulation preserved by the auditory system. By measuring threshold differences at several modulation frequencies, a modulation transfer function can be derived and used to describe the temporal response of the system. While recent studies of temporal gap detection (Eddins et al., 1992) and modulation detection (see Chapter 2) using narrowband noise have shown that temporal acuity is independent of frequency region, modified masking period patterns for broadband noise maskers have demonstrated better temporal acuity at high than low signal frequencies (e.g. Buunen, 1976). To investigate this discrepancy, the present study measured modified masking period patterns using pure-tone signals masked by narrowband and wideband noise.

Assumptions underlying the masking period pattern may be understood in terms of a simple envelope detector model often used to describe auditory processing (e.g. Rodenburg, 1977). This model incorporates an initial frequency analysis followed by an envelope extractor and an integrator. The temporal response of the system is determined by the integration stage, which is often implemented as a low-pass filter. Consider the output of the low-pass filter for an amplitude modulated noise input for very low or very high modulation frequencies. If the modulation frequency is much less than the bandwidth of the filter, then the output of the filter follows the modulated input. For modulation frequencies much greater than the filter bandwidth, the output envelope will be attenuated relative to the input, resulting in a reduced modulation depth. To describe the low-pass filter and thus the temporal properties of the system, the modulation depth at the filter output must be estimated for various modulation frequencies. The masking period pattern is used to estimate this modulation depth and to derive a modulation transfer function.

The traditional masking period pattern is obtained by measuring threshold for a short duration probe at various temporal delays relative to the period of the amplitude modulated masker. A plot of threshold as a function of delay results in a sinusoidal masking pattern corresponding to the period of modulation (e.g. Green, 1973a). Assuming that probe threshold depends upon the signal-to-masker

ratio at the output of the low-pass filter, then the threshold will vary with the modulated input. The difference between the peak and valley threshold in the masking period pattern is proportional to the modulation depth at the output of the low-pass filter.

The **modified** masking period pattern technique differs from the traditional masking period pattern in that threshold is measured only for a single long-duration probe masked by unmodulated or amplitude modulated noise rather than several short-duration probe signals masked by modulated noise. One assumption is that threshold for the long duration signal will be determined by the minima at the output of the low-pass filter, where the signal-to-masker ratio is maximal. Thus, for modulation frequencies less than the bandwidth of the low-pass filter, threshold is much lower for the modulated masker than the unmodulated masker. For higher modulation frequencies, thresholds for the modulated masker approach those for the unmodulated masker. Estimates of the modulation depth preserved by the auditory system are based upon the unmodulated minus modulated threshold difference. By using the modified technique, fewer threshold measurements are needed. Furthermore, longer duration signals have more concentrated spectra so that temporal acuity may be estimated for different signal frequencies. The relative simplicity of the task and measurement technique has lead to its use in clinical

settings as well (e.g. Zwicker, 1980; Zwicker & Schorn, 1982).

Buunen (1976) measured modified masking period patterns using 500-ms tone bursts (250 to 6000 Hz) masked by either unmodulated or amplitude modulated wideband noise. Modulation frequencies ranged from 8 to 2048 Hz. As expected, differences in threshold for the unmodulated and modulated maskers were greatest for low modulation frequencies and decreased monotonically with increasing modulation frequency. Threshold differences were greatest for signal frequencies between 2000 and 6000 Hz and decreased for signal frequencies below 2000 Hz. Buunen concluded that modulation depth was best preserved at high signal frequencies and was less well preserved below about 2000 Hz.

Zwicker (1980) further abbreviated the modified procedure by measuring threshold at only a single, relatively low, modulation frequency (14 Hz). He reported unmodulated-modulated differences of 30 dB at signal frequencies of 500, 1500, and 4000 Hz. The use of octave-band maskers, however, resulted in an eight-fold increase in bandwidth across signal frequency. Thus changes in signal frequency were confounded by changes in masker bandwidth.

To investigate inconsistencies across signal frequency and between narrowband and wideband noise, the present experiment measured modified masking period patterns for both narrowband and wideband noise maskers at four different signal frequencies.

Method

Subjects

Six subjects with normal hearing sensitivity (250 to 8000 Hz) participated in the experiment. Prior to data collection each subject completed several hours of practice on the task. Subjects were paid an hourly wage and received a 20 percent bonus upon completion of the study. Subjects S1-S3 participated in all conditions except the 800-Hz bandwidth condition. Subjects S4-S6 participated in only the 800-Hz bandwidth condition.

Stimuli

Pure-tone threshold was measured at each of four signal frequencies (500, 1000, 2000, or 4000 Hz) for four masker types: narrowband noises having bandwidths of either 200, 400, or 800 Hz, and a wideband masker (0 to 6000 Hz). The maskers were either unmodulated or sinusoidally amplitude modulated at frequencies of 4, 8, 16, 32, 64, 125, 250, or 500 Hz. The modulation frequency for a given condition did not exceed one-half the stimulus bandwidth. All stimuli were shaped with a 10 ms $\cos^2$ envelope. The total masker duration was 820 ms. The total signal duration was 410 ms and the signal was temporally centered within the masker, leaving a 205-ms fringe preceding and succeeding the signal. The masker spectrum level was 50 dB SPL. Signals were presented monaurally via headphone (Sennheiser, HD 450-13).

All stimuli were digitally generated using a digital signal processing board (TDT QAP1) and two 16 bit D/A convertors (TDT QDA1) with a sampling period of 50 μs (20,000 Hz). Broadband noises were generated by filling a 16384 point buffer with random numbers sampled from a Rayleigh distribution. The broadband noises then were filtered by setting the magnitude of the Fourier coefficients to zero outside the desired pass band. To obtain modulated noise maskers, the narrowband noises then were multiplied by the function

$$m(t) = [1 + m(\sin 2\pi Ft)] \qquad \text{Eq. 3-1}$$

where m is the index of modulation (m = 1.0) and F is the modulation frequency. All maskers were adjusted to have equivalent power. Output waveforms were low-pass filtered at 6000 Hz.

Procedure

An adaptive two-interval, two alternative forced-choice method with a three-down one-up tracking strategy was employed, estimating 79.4% correct detection (Levitt, 1971). The step size in the adaptive procedure was initially 5 dB and was reduced to 2 dB after the first three reversals. Threshold was estimated by averaging the signal level at each of the last even number of reversals, excluding the first four reversals. The final threshold for a condition was taken as the average of six 70-trial blocks. Each interval of the forced-choice trial was marked by a 820-ms light and trials were separated by

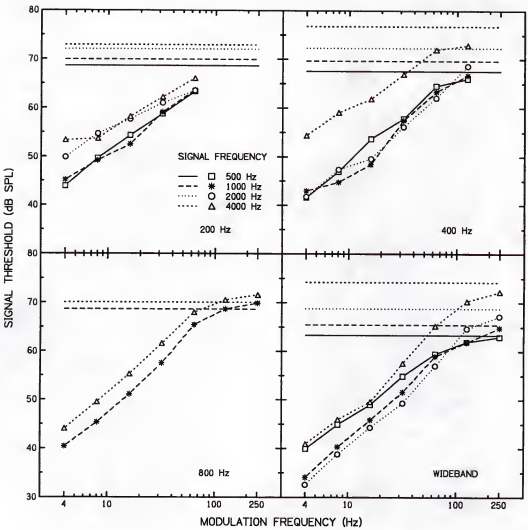

Figure 3-1. Masked threshold (mean for three listeners) as a function of modulation frequency for four bandwidth conditions. Signal frequencies are denoted by the symbols. Horizontal lines indicate threshold for unmodulated maskers and symbols connected by lines indicate thresholds for amplitude modulated maskers.

400 ms. Visual feedback was provided after each trial. Testing was conducted in a sound-attenuating chamber and stimulus timing and response collection were controlled by a microcomputer.

Results

Signal thresholds as a function of modulation frequency for the four noise bandwidths are shown in Fig. 3-1 with signal frequency indicated by the symbols. Horizontal lines at the top of each panel indicate thresholds for the unmodulated masker conditions. The data were similar across individual listeners and therefore only the mean results are shown. The standard error of the mean was about 1.5 dB for all conditions. For each bandwidth condition, thresholds for the **unmodulated** maskers (horizontal lines) increased monotonically with increasing signal frequency. This increase is consistent with the filtering properties of the auditory system, demonstrating broader tuning and therefore increased masking with increasing frequency. For a given signal frequency/masker bandwidth combination, thresholds for the **modulated** maskers were lowest for the 4-Hz modulation frequency and increased monotonically with increasing modulation frequency.

Modified masking period patterns are shown in Fig. 3-2 by plotting unmodulated minus modulated masked thresholds against modulation frequency for each of the four bandwidth conditions. The magnitude of the threshold difference

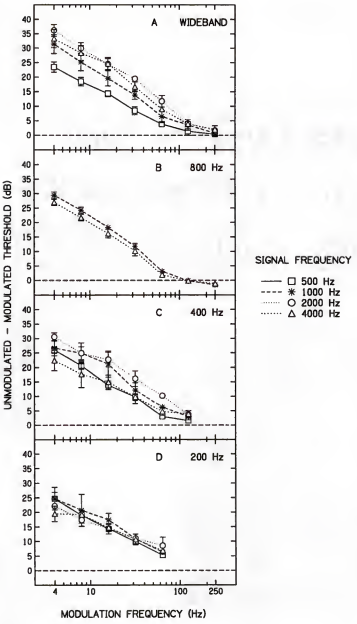

Figure 3-2. Modified masking period patterns. Unmodulated minus modulated masked threshold versus modulation frequency (mean for three listeners) for the four masker bandwidth conditions (panels A-D). Signal frequencies are indicated by the symbols. Error bars indicate the standard error of the mean. Horizontal dashed lines at 0 dB indicate unmodulated masked threshold.

reflects the ability of the auditory system to preserve the modulation depth at a particular modulation frequency. Threshold differences were greatest at low modulation frequencies and approached zero (horizontal line) as the modulation frequency increased. For the wideband maskers (panel A), the masking patterns revealed the smallest threshold differences at the 500-Hz signal frequency. The differences were progressively larger at higher signal frequencies. A repeated measures analysis of variance confirmed these results, indicating significant main effects of signal frequency ($F_{3,56}$=53.9, $p<0.01$) and modulation frequency ($F_{6,56}$=312.8, $p<0.01$). Post hoc tests (Tukey HSD) revealed significantly smaller threshold differences at 500 Hz than at other signal frequencies and smaller differences at 1000 than 2000 Hz ($p<0.05$). Threshold differences at 4000 Hz were not significantly different from those at 1000 or 2000 Hz. These results are consistent with the results reported by Buunen (1976).

Modified masking period patterns for narrowband maskers were quite different than those for wideband maskers: the threshold differences for each narrowband condition demonstrated little systematic change across signal frequency. This is clearly seen at the 800- and 200-Hz bandwidths (panels B and D). The results were more varied at the 400-Hz bandwidth (panel C), with unmodulated minus modulated differences being greatest for the 1000- and 2000-Hz signal frequencies. Statistical analyses on the

narrowband results support these observations. Repeated measures analyses of variance indicated significant main effects of frequency only for the 400-Hz bandwidth conditions ($F_{3,48}=17.24$, $p<0.05$). Post hoc tests (Tukey HSD) on the data for the 400-Hz bandwidth revealed significant differences between the 4000- and 2000-Hz signal frequencies and between the 500- and 2000-Hz signal frequencies ($p<0.05$). Thus, threshold differences did not change systematically with increasing frequency.

Discussion

Temporal Acuity

It would be useful to have a single estimate of temporal acuity for each signal frequency/masker bandwidth condition. In the context of the envelope detector model, it is assumed that the masking period pattern is determined by the low-pass filter used to represent temporal integration. Assuming that the unmodulated-modulated threshold difference is proportional to the modulation depth at the output of the hypothetical low-pass filter, a temporal modulation transfer function (TMTF) may be derived for each signal/masker condition. The derived TMTF, as in modulation detection experiments, is used to describe the temporal response of the system (e.g. Viemeister, 1979). The depth of modulation, M, "preserved" by the auditory system can be estimated from the following equation:

$$M=[(Pu-Pm)/Pu]/m \qquad \text{Eq. 3-2}$$

where Pu is threshold for the unmodulated masker, Pm is threshold for the modulated masker, and m is the modulation depth of the input (Weber, 1977). Here thresholds are in pressure units rather than dB SPL. Equation 3-2 is equivalent to the following equation given by Buunen (1976):

$$M = [\ 1 - 10\exp(-|\text{delta } T|/20)\ ]/m \qquad \text{Eq. 3-3}$$

where delta T is the unmodulated-modulated threshold difference in dB SPL. The modulation depth, M, was calculated for each modulation frequency and plotted as modulation transfer functions in dB, 20 log(M), in Fig 3-3. Each function was normalized by a constant shift such that 20 log(M) at the 4-Hz modulation frequency equaled 0 dB.

Although the transfer functions for different signal frequencies show individual variation, all functions show the typical low-pass form. Functions for the 200-Hz and 800-Hz bandwidths (panels A and C) showed little variation with signal frequency , whereas functions for the 400-Hz and wideband maskers (panels B and D) separated at high modulation frequencies, with the function for the 500-Hz signal frequency falling below the functions for the three higher signal frequencies. The low-pass form of the modulation transfer function permits a description in terms of a half-power bandwidth and an attenuation slope. For the present data, attenuation slopes in the narrowband conditions are difficult to quantify due to the limited range of modulation frequencies tested and to the non-monotonicities for the 800-Hz bandwidth. For the wideband masker, the

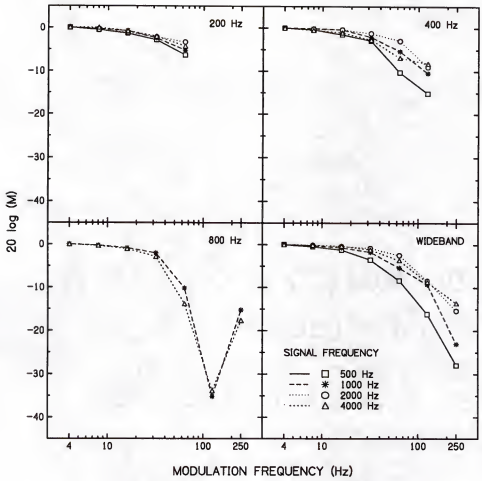

Figure 3-3. Derived temporal modulation transfer functions, modulation depth at threshold (20 log M) versus modulation frequency, based upon the unmodulated-modulated threshold differences averaged across three listeners. Panels show different bandwidth conditions with signal frequency indicated by the symbols.

attenuation slope varied from about 3 dB per doubling of modulation frequency at 4000 Hz to about 10 dB per doubling at 500 and 1000 Hz.

To estimate -3 dB bandwidths, the transfer functions were fitted with a simple low-pass filter function of the form:

$$10\log\,(1/(1+(\alpha F)^2)) \qquad \text{Eq. 3-4}$$

From this fitted function, an associated time constant was derived as $\tau=1/(2\pi F_c)$ where F_c is the -3 dB cutoff frequency. The rms error for the fitted functions was generally less than 1.0 dB except for the 800-Hz bandwidth, where the non-monotonicity led to substantially greater error. Values of τ are plotted in Fig. 3-4 for each masker/signal condition. The τ values are consistent with the trends noted in Fig. 3-3, most notably that τ changes little with signal frequency for the 200 and 800-Hz bandwidths and that τ is longer for the 500 Hz signal frequency for the 400 Hz and wideband maskers. Furthermore, the 3- to 5-ms τ values obtained from the derived MTF technique are in good agreement with the data for empirically determined MTFs as well as estimates of temporal acuity based on many other paradigms (for review, see Eddins & Green, 1993).

The above analyses indicated longer time constants at the 500-Hz signal frequency than at higher signal frequencies for both the 400-Hz and wideband masker conditions. With respect to the wideband condition, the longer time

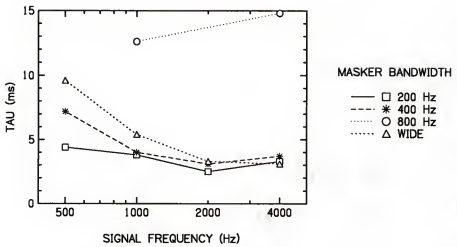

Figure 3-4. Values of τ versus signal frequency for the four masker bandwidth conditions as indicated by the symbols. Derived TMTFs (Fig. 3-3) were fitted with low-pass functions (Eq. 2-2) and values of τ were taken as $1/(2\pi f)$, where f was the -3 dB bandwidth of the fitted function.

constants at 500 Hz clearly reflect differences in the thresholds for the modulated maskers shown in Fig. 3-2 (panel A). However, for the 400-Hz bandwidth, inspection of Fig. 3-2 (panel C) reveals little difference between the 500-Hz and 4000-Hz data. In fact, the data at 500 Hz were not significantly different from 1000 or 4000 Hz.

The narrowband conditions of Zwicker and Schorn (1982) produced equally equivocal results in terms of signal frequency. They measured threshold for noise maskers that were either unmodulated or square-wave amplitude-modulated at 14 Hz. Signal frequencies were 500, 1500, and 4000 Hz and maskers were 500 Hz low-pass or octave band noises, respectively. Thus the bandwidth of the noise increased with increasing signal frequency. Unmodulated-modulated threshold differences were within 5 dB across the three conditions, with the greatest difference being at 1500 Hz. Only qualitative comparisons can be made between the present data and those of Zwicker and Schorn (1982) due to differences in stimulus conditions. Focusing on the narrowband conditions at the 16-Hz modulation frequency, the present results indicated little change in unmodulated-modulated threshold differences at 500 and 4000 Hz (<2 dB) and slightly larger differences at the two middle signal frequencies (up to 9 dB), in qualitative agreement with Zwicker and Schorn.

Comodulation Masking Release (CMR)

Formally, the conditions in this experiment are similar to conditions used in the investigation of comodulation masking release or CMR. Although the present study has focused strictly on auditory temporal acuity, it is reasonable to suspect that the across-channel processes underlying CMR may also contribute to the present results. CMR refers to the relatively lower signal thresholds that occur when the bandwidth of an amplitude modulated masker exceeds the width of a single critical band (e.g. Hall et al., 1984; see also Chapter 4 below). In this case, the modulation patterns in multiple critical bands are highly correlated and the bands are said to be "comodulated." It is believed that the auditory system is able to make across-channel comparisons of the fluctuations at different frequency regions, and the presence of a signal is easily detected as a difference in the fluctuation pattern at a single critical band.

Hall, Grose, and Moore (1993) measured pure-tone signal thresholds in unmodulated and amplitude modulated narrowband noise maskers as a function of noise bandwidth, similar to the present experiment. That experiment was designed to compare signal thresholds for maskers that were approximately one critical band wide to signal thresholds for supra-critical bandwidth maskers. Improvements in threshold for masker bandwidths wider than a single critical band were allegedly due to the across-channel processes

leading to comodulation masking release (Carlyon, Buus, & Florentine, 1989; Grose, Hall & Gibbs, 1993; Hall et al., 1993). Conditions in the latter two studies included signal frequencies of 500 and 2000 Hz, and narrowband maskers (50 and 250 Hz, Hall et al.; 76 and 240 Hz, Grose et al.) that were amplitude modulated (100%) by a 10-Hz square wave. The present study included conditions in which the masker was a 200-Hz bandwidth centered at 500 and 2000 Hz with 100% sinusoidal amplitude modulation at 8 Hz. For comparison, the present study also included a 50-Hz bandwidth centered at 500 and 2000 Hz, sinusoidally amplitude modulated (100%) at 8 Hz.

Unmodulated (UM) and amplitude modulated (AM) masked thresholds for the 50- and 200-Hz bandwidth maskers are given in Table 3-1 for the 500- and 2000-Hz signal frequencies along with the data of Hall et al. (1993) and Grose et al. (1993) for similar conditions. In addition to the raw thresholds, several threshold differences are also listed, as discussed below. Note that the masker levels were 10 dB higher in the present study than in the two previous investigations.

First the data will be considered in terms of temporal acuity, and then in terms of possible across-channel processes. Following the abbreviated measure used by Zwicker and Schorn (1980), thresholds for the modulated maskers were subtracted from those for the unmodulated maskers, and are given in the rows labeled "MOD DIFF." For the present

Table 3-1. Pure-tone thresholds (dB SPL) in unmodulated (UM) and amplitude modulated (AM) narrowband masking noise. Results are shown for the present experiment and for the experiments of Hall et al. (1993) and Grose et al. (1993). Data are presented for signal frequencies of 500 and 2000 Hz and two noise bandwidths at each signal frequency. Rows labeled MOD DIFF give corresponding UM minus AM values. Columns labeled BW DIFF give threshold differences between the wide and narrow masker bands.

Signal Frequency	500 Hz			2000 Hz			
Present Data							
	50 Hz	200 Hz	BW DIFF	50 Hz	200 Hz	BW DIFF	Potential CMR
UM (dB)	68.7	68.6		68.0	72.0		
AM (dB)	58.1	49.6	8.5	58.9	54.7	4.2	4.3
MOD (dB) DIFF	10.6	19.0		9.1	17.3		
Hall et al. (1993)							
	50 Hz	250 Hz	BW DIFF	50 Hz	250 Hz	BW DIFF	Potential CMR
UM (dB)	59.4	60.2		58.8	64.4		
AM (dB)	41.0	32.3	8.7	39.7	38.9	0.8	7.9
MOD (dB) DIFF	18.4	27.9		19.1	25.5		
Grose et al. (1993)							
	76 Hz	240 Hz	BW DIFF	76 Hz	240 Hz	BW DIFF	Potential CMR
UM (dB)	62.0	63.0		61.5	64.0		
AM (dB)	42.2	33.0	9.2	48.8	41.1	7.7	1.5
MOD (dB) DIFF	19.8	30.0		12.7	22.9		

data and those of Hall et al., these differences were nearly the same for the 500 and 2000-Hz signal frequencies at each bandwidth. This may be interpreted as indicating similar temporal acuity at the two signal frequencies. The data of Grose et al. (1993) show smaller differences at 2000 Hz than at 500 Hz, suggesting slightly poorer temporal acuity at the higher frequency region.

Now consider the data in terms of possible across-channel processes. For the unmodulated (UM) maskers of the present experiment, thresholds at the 500-Hz signal frequency were nearly the same for the narrow and wide bandwidths (68 dB). This is consistent with the fact that energy outside the critical band surrounding the signal contributes little to masking. At 2000-Hz, however, thresholds increased from the 50- to the 200-Hz bandwidth (68 to 72 dB), reflecting an increase in masker energy within a single critical band centered at 2000-Hz.

Thresholds for the modulated (AM) conditions, however, actually decreased from the 50- to the 200-Hz bandwidth. The threshold difference between the 200- and 50-Hz bandwidths, shown in the "BW DIFF" column, was 8.5 dB for the 500-Hz signal. It is possible that across-channel processes contributed to the 8.5 dB change at the 500-Hz signal frequency, since the 200-Hz bandwidth was wider than a single critical band. For the 2000-Hz signal, the difference in the modulated conditions was only 4.2 dB. At this frequency, both maskers were less than a critical band

wide, so it is unlikely that the 4.2-dB threshold difference was due to across-channel processes. A conservative estimate of the potential CMR, as listed in Table 3-1, may be obtained by subtracting the threshold difference between bandwidth conditions at the two frequencies (8.5 - 4.2 = 4.3 dB CMR). Evaluation of the two previous studies (Table 3-1) reveals the same general trends.

One interpretation of the present data, therefore, is that the difference in threshold between unmodulated and modulated maskers is due in part to the temporal resolution of the auditory system and in part, at least in some conditions, to mechanisms underlying across-channel envelope comparisons. The results for the wideband masker are difficult to explain in terms of CMR mechanisms. Evidence from previous investigations suggest only slight differences in CMR with signal frequency (e.g. Schooneveldt & Moore, 1987), while the present data indicate substantial differences with changing signal frequency.

Conclusions

The present study employed a modified masking period pattern technique to estimate temporal resolution as a function of signal frequency. The results were different for narrowband and wideband noise maskers. For narrowband noise maskers, derived estimates of temporal acuity indicated little systematic change with changes in signal frequency. These results are generally consistent with

previous investigations of temporal acuity in which gap detection (e.g. Eddins et al., 1992) and modulation detection (see Chapter 2) were measured for narrowband noise stimuli. For a wideband noise masker, however, the derived estimates indicated better temporal acuity at high than low signal frequencies. Several masker conditions were similar to those used in investigations of comodulation masking release. Thresholds for those conditions are consistent with previous CMR studies.

CHAPTER 4
ACROSS-CHANNEL TEMPORAL PROCESSING: COMODULATION MASKING RELEASE FOR UN-MODULATED AND SINUSOIDALLY AMPLITUDE MODULATED STIMULI

Introduction

Consider the detection of a signal centered in a narrowband masker. The signal is easier to detect if other parts of the audio spectrum contain energy having envelope spectra coherent with the narrowband masker. These remote maskers are said to be comodulated with the masker at the signal frequency, and the resulting decrease in threshold is termed comodulation masking release or CMR (e.g. Hall et al., 1984; Hall, 1987). It is generally believed that CMR results from a comparison of the stimulus envelopes across different frequency regions. If the envelopes are incoherent across frequency, then the addition of a signal has little influence on their relation. If, however, the envelopes are coherent across frequency, the addition of signal renders the envelope in the signal region incoherent with those from other frequency regions. It is this difference in envelope coherence that aids signal detection.

Two common masking paradigms have been used to measure CMR. The first involves a comparison of pure-tone thresholds masked by either unmodulated or amplitude modulated noise. Here, detection is easier for the amplitude modulated masker, due to the coherent envelopes across

frequency. In the second paradigm, the signal is masked by a single narrowband noise centered on the signal frequency or by the same noise with flanking noise bands having either the same envelope (coherent noise) or different envelopes (incoherent noise). The addition of incoherent noise has little effect on thresholds, whereas the addition of coherent noise reduces the signal threshold.

A primary determinant of CMR magnitude is the rate of envelope fluctuation: CMR decreases with increasing fluctuation rate. This occurs both when the fluctuation rate is changed by varying the rate of amplitude modulation of a broadband noise (Hall & Haggard, 1983; Buus, 1985; Hall, 1987; Hall, Cokely, & Grose, 1988; Schooneveldt & Moore, 1988a; Moore & Schooneveldt, 1990) or by changing the bandwidth of multiple narrowband noise maskers (Hall, 1986; Schooneveldt & Moore, 1987, 1988a; Hall et al., 1988; Haggard, Hall, & Grose, 1990; Moore & Schooneveldt, 1990). The purpose of the present investigation was to determine how the threshold of a tonal signal, and thus the magnitude of the CMR, is influenced by multiple narrowband noise maskers that incorporate two separate rates of envelope fluctuation, a fast rate determined by the noise bandwidth and a slow rate determined by sinusoidal amplitude modulation (SAM).

In combining two rates of fluctuation simultaneously, two results seem plausible. Given that the magnitude of the CMR increases as the fluctuation rate decreases, it is

possible that signal detectability will be determined solely by the pattern of the slowest envelope fluctuations across bands. In this case, the magnitude of the CMR would depend only upon the across-band coherence of the SAM and would not be influenced by the coherence of the noise carriers.

A second possibility is that signal detectability will be determined by both the slow and the fast envelope fluctuations. Accordingly, the magnitude of the CMR would be determined primarily by the across-band coherence of the SAM, but would increase further from coherence of the noise bands.

The results of three experiments are reported. In the first experiment, the effect of a single rate of envelope fluctuation on CMR was investigated by varying either the bandwidth of multi-band noise maskers or by varying the rate of SAM for tonal-complex maskers. In the second and third experiments, CMR was measured for multi-band SAM noises to determine the relative contributions of slow and fast modulation rates. In Exp. 2 the signal was a 500-ms pure tone and in Exp. 3 the signal was a train of tone-pulses temporally centered at either a peak or a valley of the modulation cycle.

General Method

Subjects

Three paid subjects (S1-S3) and author DAE (S4) participated in this project. All had normal hearing sensitivity (250 to 8000 Hz) and ranged in age from 20-28 years. Each listener received several hours of training on a variety of CMR conditions with both unmodulated and amplitude-modulated noise bands prior to data collection. The paid subjects received an hourly wage and were given a 20% bonus upon completion of the project.

Procedure

An adaptive two-interval, two-alternative forced-choice method with a three-down, one-up tracking strategy was used to estimate 79.4% correct detection (Levitt, 1971). The step size in the adaptive procedure was initially 5 dB and was reduced to 2 dB after the first three reversals. Threshold was estimated by averaging the signal level at each of the last even number of reversals, excluding the first four reversals. The final threshold for a condition was taken as the average of six 60-trial blocks. Each observation interval was marked by a 500-ms light and visual feedback was provided after each trial. Testing was conducted in a sound-attenuating chamber and stimulus timing and response collection was controlled by a microcomputer.

Experiment 1. Single Fluctuation Rate

Introduction

Previous investigations showing that CMR increases with decreasing masker fluctuation rate have employed either two narrowband noises or an amplitude-modulated broadband noise, and have used only a small number of envelope fluctuation rates. In this experiment, the influence of fluctuation rate on the magnitude of CMR for multiband (5) maskers was investigated. Envelope rate was systematically varied by manipulating either the bandwidth of each constituent narrowband noise or the modulation rate of each constituent tone. If CMR is primarily determined by the envelope fluctuation rate, then similar results should be obtained for both stimulus types. The results provide a baseline for evaluating the contribution of each individual rate when two rates are simultaneously present (Exps. 2 and 3).

Stimuli

The signal was a pure tone at 2500 Hz. Noise maskers consisted of five narrowband noises and tonal maskers consisted of five sinusoidal carriers. For both masker types, the five maskers had center frequencies of 1500, 2000, 2500, 3000, and 3500 Hz. For unmodulated narrowband noise, the envelope fluctuation rate was defined as the number of envelope maxima per second, which may be approximated as

$$N = 0.64110(f_b - f_a) \qquad \text{Eq. 4-1}$$

where f_b is the lower-cutoff frequency and f_a is the upper-cutoff frequency of the noise band (Rice, 1954). For SAM tones, the fluctuation rate was defined as the frequency of modulation. The width of each narrowband noise was either 10, 16, 20, 50, 100, or 200 Hz. There were two noise conditions. The noises either had the same temporal envelope across bands (coherent condition), or different temporal envelopes across bands (incoherent condition). The "noise CMR" was calculated as the threshold for the incoherent condition minus that for the coherent condition. For the tonal maskers, the rate of SAM was either 10, 13, 20, 34, 64, or 128 Hz. These rates correspond to the envelope fluctuation rate of the narrowband noise maskers (i.e. 0.64 · bandwidth). In the two SAM conditions, the phase of the SAM was either the same across the tones (phase-coherent condition) or was successively shifted by $2\pi/5$ radians across the tones (phase-incoherent condition). The "SAM CMR" was calculated as the phase-incoherent threshold minus the phase-coherent threshold. The signal and the masker were always gated synchronously for a total duration of 500 ms, including 10-ms $\cos^2$ rise/fall envelopes. The masker spectrum level was 50 dB SPL for the noise-band maskers and 70 dB SPL for the tonal maskers.

All stimuli were digitally generated using a digital signal processing board (TDT QAP1) and two 16-bit D/A converters (TDT QDA1) with a sampling period of 61 μs (16393 Hz). Noise maskers were generated by filling a

portion of an 8192-point buffer with randomly selected amplitudes (Rayleigh) and a second buffer with randomly selected phases (uniform). A subsequent inverse FFT on the magnitude and phase buffers yielded the desired noise band. On each observation interval, the five masker bands were generated separately, equalized in energy, and summed to form the composite masker delivered to the listener via headphone (Sennheiser HD 250-13). For incoherent noise, different temporal envelopes were obtained by drawing independent sets of magnitudes and phases for each of the five center frequencies. For coherent noise, the same temporal envelope was obtained by drawing one set of magnitudes and phases that was duplicated at each of the five center frequencies.

The same technique was used to generate tonal maskers, but with only a single amplitude and phase drawn for each of the five tones. For SAM conditions, the time waveform of the i^{th} tone was multiplied by the function

$$M_i(t) = [1 + m(\sin 2\pi Ft + \theta_i)] \qquad \text{Eq. 4-2}$$

where m is the modulation depth, F is the modulation frequency, and θ_i is the phase of the i^{th} modulator. The modulation depth was always 100% (m = 1). A single value of θ was randomly chosen on each presentation interval. For the phase-coherent conditions, the value of θ was the same across all five bands. For the phase-incoherent conditions, the value of θ was successively shifted by

$2\pi/5$ radians for each of the five bands. The signal was presented in phase with the on-frequency carrier.

Results and Discussion

Signal thresholds are plotted in Fig. 4-1 for the noise maskers (squares) as a function of bandwidth (upper abscissa) and for the SAM tonal maskers (circles) as a function of SAM rate (lower abscissa). Note that the data are plotted so that SAM rate corresponds to 0.64 times the noise bandwidth, thereby equating fluctuation rate for the two masker types. Each point represents the mean threshold across listeners S1-S3. Listener S4 (DAE) did not participate in this experiment. For both masker types, thresholds were consistently lower for the coherent (filled symbols) than the incoherent (open symbols) conditions, demonstrating a CMR at each bandwidth and SAM rate.

For the noise maskers, threshold increased with increasing bandwidth for the incoherent and coherent conditions. This increase was presumably due to the addition of energy in the frequency region surrounding the signal (e.g. Fletcher, 1940; Hall et al., 1984). Thresholds in the incoherent condition increased by 1.9 dB per doubling of bandwidth, which is close to the 1.5-dB increase expected from an energy detector (Green, 1960; Spiegel, 1981). Coherent thresholds increased at a rate of 3.7 dB per doubling of bandwidth. Hall (1986) has suggested that the relatively steep threshold improvement for coherent-noise

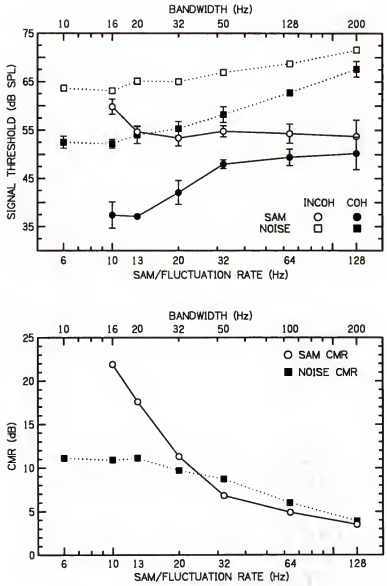

Figure 4-1. Upper panel: signal threshold (dB SPL) versus modulation frequency for the tonal maskers (lower abscissa; circles) or bandwidth for the noise maskers (upper abscissa; squares). Note that the data are scaled in terms of fluctuation rate (fm = 0.64 times noise bandwidth). Open symbols are for incoherent maskers and filled symbols indicate coherent maskers. Lower panel: CMR values versus noise bandwidth or modulation frequency using the same axes as in the upper panel. SAM CMRs are indicated by the open circles and noise CMRs by the filled squares.

maskers is due not only to an increase in masker energy surrounding the signal but also to an increase in the envelope fluctuation rate with increasing bandwidth. For the SAM tonal maskers, thresholds were relatively constant across SAM rate in the incoherent condition, but increased with increasing SAM rate in the coherent condition.

CMR magnitude is plotted as a function of fluctuation rate in the bottom panel of Fig. 4-1 for both narrowband noise (filled squares) and tonal maskers (open circles). The upper and lower abscissas are the same as the upper panel. For both masker types, CMR magnitudes decreased with increasing fluctuation rate, confirming previous reports (Hall & Haggard, 1983; Hall, 1986; Schooneveldt & Moore, 1987, 1990; Hall et al., 1988; Haggard et al., 1990; Moore & Schooneveldt, 1990). Measurable CMRs values persisted to the highest rate tested (128 Hz).

At fluctuation rates of 20 Hz and greater, CMR values were about the same for both masker types. However, for slower fluctuation rates, SAM CMRs were considerably larger than the noise CMRs. The larger SAM CMRs may be due to the more pronounced envelope minima and to the greater envelope regularity for SAM tonal maskers than for noise maskers.

Experiment 2. Two Fluctuation Rates: 500-ms Signal

Introduction

In the second experiment, multiple narrowband noises having relatively fast inherent envelope fluctuation rates

were sinusoidally amplitude modulated at a slow rate. The masker thus contained two rates of envelope fluctuation simultaneously. The experiment tested whether CMR was primarily determined by the slowest fluctuation rate or whether the two rates contributed separately to the magnitude of CMR.

Stimuli

The masker was composed of five noise bands centered at 1500, 2000, 2500, 3000, and 3500 Hz, the same center frequencies used in Exp. 1. The width of each band was always 100 Hz, corresponding to an average envelope rate of 64 Hz. The rate of SAM was always 10 Hz. Figure 4-2 shows sample waveforms and coding symbols for each noise condition. For clarity, the sample duration is 250 ms and only the outermost bands are pictured (1500 and 3500 Hz). Each symbol is composed of a bottom half denoting the noise condition, and a top half denoting the SAM condition. The noise maskers were incoherent (I) in the three conditions shown in the top row, and were coherent (C) in the three conditions shown in the bottom row. These maskers were presented under three different SAM conditions. There was either no modulation (NM, left column), phase-incoherent modulation (PI, center column), or phase-coherent modulation (PC, right column). Data in SAM conditions were also collected using tonal carriers.

Noise, SAM, and combined CMRs were calculated. A "noise CMR" was calculated as the incoherent-noise

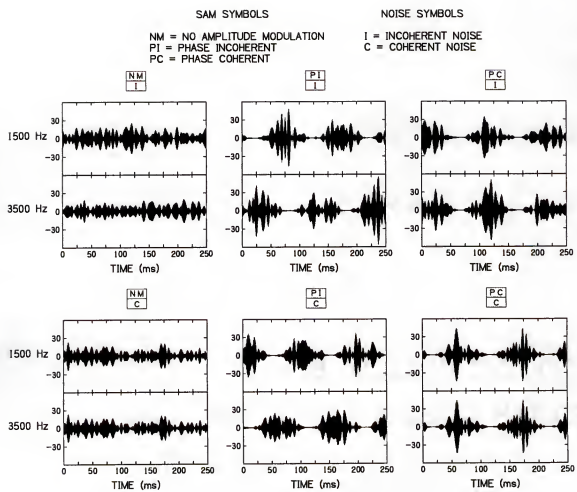

Figure 4-2. Sample waveforms for the six noise masker conditions of Exp. 2. 250-ms samples are shown for the lowest- (1500) and highest- (3500) frequency masker bands in each condition. Above each waveform pair is a symbol denoting the masker condition. The upper portion of the symbol indicates the modulation type (NM, no modulation; PI, phase-incoherent modulation; PC, phase coherent modulation) and the lower portion indicates the noise carrier type (I, incoherent noise; C, coherent noise).

threshold minus the coherent-noise threshold for a given type of amplitude modulation. Likewise, a "SAM CMR" was calculated as the phase-incoherent threshold minus the phase-coherent threshold for a given type of noise carrier. Finally, a "combined CMR" was calculated by comparing conditions in which the coherence across conditions differed at both rates.

For an unmodulated masker, thresholds are nearly the same for a single-band masker as for multi-band incoherent maskers. When the maskers are amplitude modulated, however, threshold for a phase-incoherent multi-band masker may be much higher than for the single modulated band (Grose & Hall, 1989; Moore, Glasberg, & Schooneveldt, 1990). In that case CMR should be defined in two ways: 1) the phase-incoherent minus the phase-coherent masked threshold, and 2) the single-modulated-band threshold minus the phase-coherent masked threshold. Therefore, signal thresholds were also measured for three single-band masker conditions: an unmodulated noise, a SAM noise, and a SAM tone. Noise, SAM, and combined CMRs were then calculated as the threshold for the single band masker minus the multi-band masked threshold.

Stimuli were generated as in Exp. 1 except that SAM was applied to both the noise and the tonal carriers. The spectrum level of the noise maskers was 50 dB SPL in both the SAM and no-SAM conditions.

Results

Noise CMR

Signal thresholds in the left section of Fig. 4-3 are plotted to reveal the three noise CMRs, one for each of the SAM conditions. Each point is the mean threshold for four listeners (S1-S4). The standard error of the mean computed across data for individual listeners was approximately 0.9 dB for all conditions depicted in the figure. The magnitude of each CMR is listed at the bottom of the figure.

With no SAM present (comparison NM), the mean threshold was 68.7 dB for the incoherent noise (NM/I) and was 62.4 dB for the coherent noise (NM/C), yielding a noise CMR of 6.3 dB. For the phase-incoherent conditions (comparison PI), thresholds were also higher for the incoherent noise (PI/I, 65.1 dB) than for the coherent noise (PI/C, 61.6 dB), yielding a noise CMR of 3.5 dB. Finally, for the phase-coherent conditions (comparison PC), thresholds were again higher for the incoherent noise (PC/I, 47.2 dB) than the coherent noise (PC/C, 41.9 dB), resulting in a noise CMR of 5.3 dB. Therefore, a noise CMR of similar magnitude was obtained in all three SAM conditions, averaging 5.0 dB across conditions. Amplitude modulation of the noise lowered thresholds by about 5 dB for the phase-incoherent conditions and about 20 dB for the phase-coherent conditions.

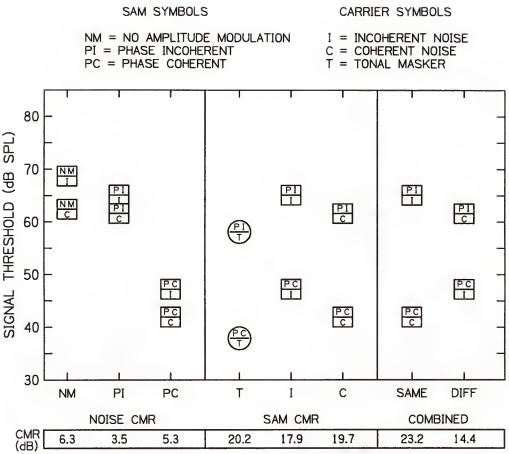

Figure 4-3. Signal threshold versus various masker comparisons. The symbols indicate masker conditions as in Fig. 4-2. Below each comparison, an associated CMR value is given. The squares indicate data from Exp. 2. The circles represent the tonal masker conditions of Exp. 1 for a 10-Hz SAM rate. Note that data for S4 have been added to data from Exp. 1. The data are plotted to reveal NOISE CMRs (left), SAM CMRs (middle), and COMBINED CMRs (right). The squares in the middle and right sections are replotted from the left section.

SAM CMR

The middle section of Fig. 4-3 shows signal thresholds plotted to reveal three SAM CMRs, one for tonal carriers and two for noise carriers. The tonal conditions (circles, comparison T) are identical to those of Exp. 1 (10-Hz SAM), but data for S4 have been added. Thresholds for the modulated noise maskers (PI/I, PI/C, PC/I, and PC/C) are replotted from the left section of Fig. 4-3. For all three comparisons, signal thresholds were higher for the phase-incoherent conditions than the phase-coherent conditions. The mean threshold was 58.1 dB for the phase-incoherent tonal masker (PI/T) and 37.9 dB for the phase-coherent tonal masker (PC/T), yielding a SAM CMR of 20.2 dB. The SAM CMR was 17.9 dB for incoherent noise (comparison I) and 19.7 dB for coherent noise (comparison C). Thus the three SAM CMRs had a similar magnitude, averaging 19.3 dB.

Combined CMR

To illustrate the combined effects of noise and SAM CMRs, two additional CMRs were calculated from this data. Data in the left section of Fig. 4-3 are replotted in the right section to reveal these combined CMRs. A comparison of conditions in which the bands were the same at both rates, either coherent (PC/C) or incoherent (PI/I), yielded an augmented CMR of 23.2 dB (comparison SAME). In this comparison, the noise and the SAM CMRs combined to yield a greater CMR than either the noise or SAM CMR alone. Likewise, a comparison of conditions in which the bands were

different at the two rates, coherent at one rate and incoherent at the other (PC/I and PI/C), resulted in a diminished CMR of 14.4 dB (comparison DIFF). Thus the amount of masking release depended upon the temporal information at both fluctuation rates, and coherence at both rates lead to greater masking release than either rate alone.

Single-band CMR

Figure 4-4 shows signal thresholds for the single-band and multi-band conditions plotted to reveal single-band CMRs. Each point is the mean threshold for four listeners (S1-S4). The multi-band thresholds are re-plotted from Fig. 4-3. The magnitude of each single-band CMR is listed at the bottom of the figure.

Mean threshold for the single-band masker was 66.0 for the unmodulated noise (NM, shaded rectangle), 45.6 for the SAM tone (AM, shaded circle), and 52.2 for the SAM noise (AM, shaded rectangle). For the noise and SAM CMRs (left and middle sections) only a single rate of fluctuation was present. The addition of coherent flanking bands always reduced threshold (comparisons C and PC), yielding positive CMRs. In contrast, adding incoherent flanking bands always increased threshold (comparisons I and PI), yielding negative CMRs. The magnitude of the SAM CMR was always larger than that for the noise CMR.

When two rates of fluctuation were present (combined CMRs), adding coherent SAM (DIFF1 and SAME2 comparisons) always produced a positive single-band CMR, whereas adding

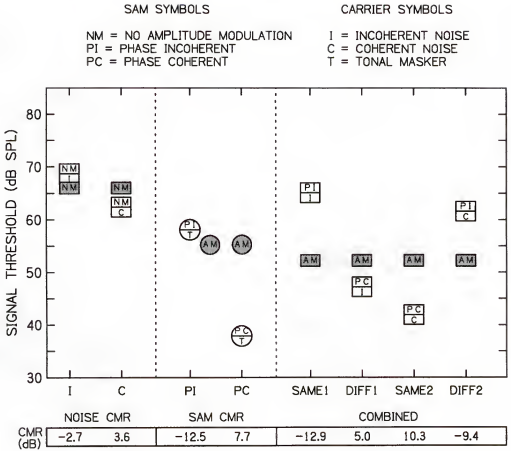

Figure 4-4. Signal thresholds for multi-band (open symbols) and single-band (shaded symbols) maskers. The data are plotted as in Fig. 4-3.

incoherent SAM (SAME1 and DIFF2 comparisons) always yielded a negative single-band CMR. Further, thresholds were always lower for the coherent than the incoherent noise carriers for a given SAM condition. Thus, the sign of the CMR was determined by the coherence of the slow fluctuations (SAM) but the magnitude of the CMR also depended upon the fast fluctuations (noise).

Discussion

The results of the present experiment are consistent with the idea that signal detectability is determined by both the slow and the fast envelope fluctuations. This held true for both the phase-incoherent reference and the single-band reference. The notion that CMR is determined solely by the pattern of the slowest fluctuations across masker bands is not tenable given the present data.

The magnitude of the "noise CMR" was about 5 dB regardless of the presence or absence of amplitude modulation, and regardless of the across band coherence of the SAM when present. Consistent with this result, McFadden (1987) reported CMRs of 3 to 7 dB using unmodulated noise similar to the present NM conditions. The "SAM CMR" was about 19 dB for all three carrier types, similar in magnitude to SAM CMRs reported previously for tonal carriers (Grose & Hall, 1989; Moore et al., 1990). "Combined CMRs" revealed a novel result, indicating that the magnitude of the CMR was dependent upon both the across-band coherence

of the SAM and the coherence of the noise bands. Apparently, the auditory system is able to combine the slow and the fast fluctuation cues. One remarkable demonstration of this was the noise CMR obtained the phase-incoherent SAM conditions. Here, despite the slow amplitude modulation of the noise envelope at different modulation phases, the auditory system was able to extract across-frequency information from the noise carrier which enhanced detection.

Theory

Several mechanisms have been suggested to account for CMR, generally falling into one of two categories. The first category involves a comparison of the pattern of envelope fluctuations across multiple frequency channels. One example of such a mechanism has been explored by Richards (1987) and is based on the correlation of envelopes from disparate frequency regions.

Richards (1987) noted that monaural envelope discrimination was similar to CMR and suggested that the two might result from the same process. She proposed a model in which the envelopes of the noise bands to be discriminated are first extracted and then a correlation of the envelopes is calculated. In the case of coherent noise, the envelopes from different frequency regions are highly correlated and the addition of a signal at one frequency serves to de-correlate the envelopes. For incoherent noise, the envelopes are uncorrelated initially and the

addition of a signal has little effect on the correlation. It is thought that the de-correlation in the coherent case leads to a masking release. A second envelope pattern model closely related to envelope correlation model is the equalization-cancellation model (Buus, 1985; Hall, 1986). This model similar to the model by Durlach (1963) for the binaural masking level difference. Green (1992) has shown that decision rules based on the envelope correlation and the equalization-cancellation models are monotonically related, and suggested that the two models may be treated as essentially the same.

To evaluate the present results in terms of an envelope correlation model, a series of simulations were run following the model of Richards (1987). For each masker condition, correlations and r to z transformations were calculated among the on-frequency and flanking band envelopes both with and without the signal present at threshold level. The results indicated that the change in z produced by the addition of a signal at threshold level was not constant across conditions, as predicted by the model. The reader is cautioned not to reject Richards' model based on these results. That model was based on correlations obtained with unmodulated narrowband noise, whereas the present stimuli consisted of amplitude modulated noise and tonal carriers. Here, no additional assumptions or modifications to the model were made to account for stimulus differences. The simulations do

indicate that thresholds in the present CMR conditions cannot be explained by simple changes in envelope correlation with the addition of a signal.

A second class of model for CMR is based on a strategy of listening in the valleys or the "dips" of the masker. This model proposes that the envelope fluctuations of the comodulated flanking bands cue the listener to the occurrence of minima in the single on-frequency masker band, where the signal-to-masker ratio is greatest (Buus, 1985). By giving relatively more weight to information in the masker minima, the improved signal-to-masker ratio would enhance detection. In terms of the present data, this "cued temporal listening" model is attractive. Such a model is consistent with the results of Exps. 1 and 2. Slower envelope fluctuations are marked by relative well defined minima, and thus flanking bands could better indicate the time at which the signal-to-noise ratio is most favorable. It was precisely the conditions having these slow envelope fluctuations that resulted in the largest CMRs (e.g. low SAM rates and narrow noise bandwidths). Because sinusoidal amplitude modulation is periodic, envelope minima might be identified with more precision than for narrowband noise, leading to larger CMRs than noise maskers have approximately the same envelope rate. This was evident in the data of both experiments.

Furthermore, the envelopes of phase-coherent noise have minima corresponding to SAM and secondary minima

corresponding to the noise carriers. Inspection of the waveform in the lower right section of Fig. 4-2 reveals a secondary minimum corresponding to about 70 ms. In the case of phase-incoherent SAM, it is possible that the across-band coherence of these secondary minima give rise to a noise CMR despite the incoherence of the SAM. Thus it appears that the data of the present experiment support the cued temporal listening model.

Experiment 3. Two Fluctuation Rates: Pulse-Train Signal With Peak and Valley Signal Placement

Introduction

In a variant of the standard CMR paradigm, Grose and Hall (1989) and Moore et al. (1990) measured CMR for brief tone-pulse signals temporally centered at either a peak or a valley of a SAM tonal masker. They reported CMRs of 10 to 28 dB for signals located in the masker valleys. For peak signal placement, however, the phase-coherent thresholds were actually higher than both the phase-incoherent and single-band thresholds, yielding CMRs of -4 to -7 dB. The results of Exp. 2, indicating that noise and SAM CMRs could be obtained separately, opened the possibility that a noise CMR might be obtained for peak signal placement even in the absence of a SAM CMR. A CMR for peak signal placement, however, would be inconsistent with a strategy based upon cued temporal listening. Thus, in the final experiment, CMR was measured for peak and valley signal placement using maskers having two rates of envelope fluctuation.

Stimuli

Masker conditions and stimulus generation were identical to those of Exp. 2. However, here the signal was a train of three tone pulses each having a total duration of 50 ms, including a 10-ms $\cos^2$ rise/fall envelope. The inter-pulse interval was 50 ms. The 500-ms masker was modulated at 10 Hz and thus contained five cycles of modulation. For SAM conditions, each pulse train was temporally centered in either a peak or a valley of the 2500-Hz masker band. The pulse train always began in the second modulation cycle and ended in the fourth modulation cycle. Because the starting phase of modulation of the 2500-Hz band was random from trial to trial, the delay to signal onset varied across trials. For conditions with no SAM, the pulse train was temporally centered within the 500-ms masker, having a 125-ms masker fringe before and after the signal.

Results

Peak signal placement

Thresholds for peak signal placement are shown in Fig. 4-5 in the same manner as in Fig. 4-3. The results in the left section of Fig. 4-5 are plotted to reveal noise CMRs. For unmodulated noise (comparison NM), thresholds were 78.1 dB for the incoherent noise (NM/I) and 72.2 dB for the coherent noise (NM/C). These values are about 10 dB higher than for the 500-ms signal of Exp. 2. The noise CMR of 5.9

dB was in good agreement with the 6.3-dB noise CMR obtained for the 500-ms signal. For the phase-incoherent condition (comparison PI), peak signal threshold was 80.9 dB for the incoherent noise (PI/I) and 80.7 dB for the coherent noise (PI/C), indicating no noise CMR. For the phase-coherent condition (comparison PC), peak signal threshold was 80.8 dB for incoherent noise (PC/I) and was 78.6 dB for coherent noise (PC/C), yielding a modest noise CMR of 1.8 dB.

Results are plotted in the middle section of Fig. 4-5 to reveal SAM CMRs. The noise data are replotted from the left section of the figure. For tonal carriers (comparison T), threshold was 66.4 dB for the phase-incoherent condition (PI/T) and 66.0 dB for the phase-coherent condition (PC/T), revealing no CMR. Similarly, for incoherent noise carriers (comparison I), no threshold difference was found. For coherent noise carriers (comparison C), threshold was slightly higher for the phase-incoherent than the phase-coherent condition, yielding a modest SAM CMR of 2.1 dB. For completeness, the combined CMRs are plotted in the right section of Fig. 4-5. The magnitude of these CMRs was quite small due to the noise and SAM CMRs.

Figure 4-5 also shows thresholds for the single-band maskers (shaded symbols). No data were collected for the unmodulated single-band masker. Threshold for the single-band SAM noise masker was 72.6 dB (AM, shaded rectangle), about 5 to 7 dB lower than each of the multi-band SAM maskers (comparisons PI and PC). Threshold was 60.8 dB for

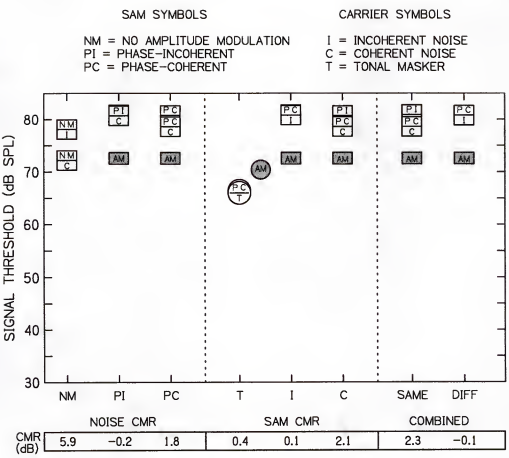

Figure 4-5. As for Fig. 4-3 but with pulse-train signals temporally located within a masker peak. Shaded symbols indicate single-band masked thresholds.

the single-band SAM tonal masker (AM, shaded circle), about 5 dB lower than the multi-tonal SAM maskers. Thus, peak signal placement resulted in negative single-band CMRs for all conditions, similar to the results of Grose and Hall (1989) and Moore et al. (1990).

Valley signal placement

Thresholds for valley signal placement are shown in Fig. 4-6. The results were similar in form to those obtained with the 500-ms signal (Exp. 2), but the CMRs tended to be larger. Thresholds for the unmodulated noise are replotted from Fig. 4-5. Thresholds for the phase-incoherent conditions (comparison PI) were generally about 6 dB higher than those for the 500-ms signal, while thresholds for the phase-coherent conditions (comparison PC) were about the same as those for the 500-ms signal. The three noise CMRs averaged about 5 dB, similar to those for the 500-ms signal. The three SAM CMRs, however, were about 6 dB larger for the pulse-train than the 500-ms signals, averaging about 25 dB. The larger SAM CMRs were primarily due to higher phase-incoherent thresholds. This led to combined CMRs that were about 5 dB larger for pulse-train signals presented in the masker valleys than for 500-ms signals.

Single-band threshold for valley signal placement was 55.1 dB for the SAM noise (AM, shaded rectangles) and 48.9 dB for the SAM tonal maskers (AM, shaded circles). This was about 3 dB higher than for the 500-ms signal in both

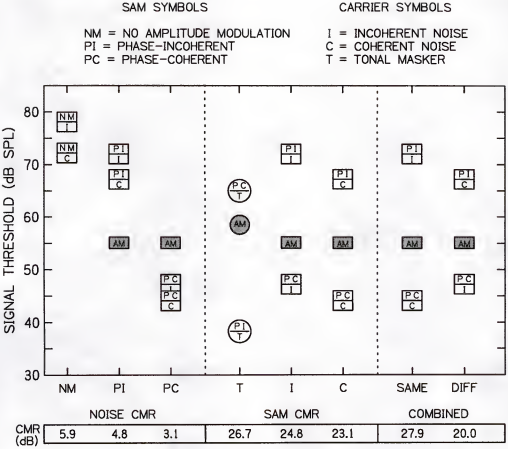

Figure 4-6. As for Fig. 4-3 but with pulse-train signals temporally located within a masker valley. Shaded symbols indicate single-band masked thresholds.

conditions. The single-band CMRs were about 10 dB in comparisons involving phase-coherent conditions and about -14 dB in comparisons involving phase-incoherent conditions. Thus, the single-band CMRs for valley signal placement were about 3 dB greater in magnitude than the corresponding CMRs for the 500-ms signal.

Discussion

For peak signal placement, both noise and SAM CMRs were small or absent for the multi-band reference. The lack of a substantial SAM CMR for peak placement is consistent with previous reports for tonal carriers, although those studies typically indicated small negative SAM CMRs for peak placement (Grose & Hall, 1989; Moore et al., 1990). It is evident that processes leading to a CMR are greatly impaired when the signal is placed in the masker peaks. Perhaps a requirement for CMR is that the some portion of signal be located in the masker valleys. An envelope correlation model, however, would predict a masking release for peak signal placement as well as valley signal placement. In both cases, the addition of a signal would reduce the across-band envelope correlation for maskers with coherent envelopes. Since no CMR occurred for peak signal placement in the present experiment as well as in the experiments by Grose et al. (1989) and Moore et al. (1990), an explanation based upon across-frequency envelope

correlation would be insufficient to account for the results.

The present data are consistent with a cued temporal listening model, which holds that the presence of coherent flanking bands cue the listener as to the temporal location of the masker valleys. By listening in these valleys, an optimal signal-to-masker ratio may be obtained. The present CMR results for valley signal placement are largely consistent with the results of Exp. 2 for a 500-ms signal.

The addition of incoherent flanking bands to the 2500-Hz band generally led to an increase in masking, and corresponding negative single-band CMRs. Similar interference effects have been noted previously for narrowband noise maskers and for SAM tonal maskers (Hall et al., 1984; McFadden, 1986; Cohen & Schubert, 1987; Schooneveldt & Moore, 1987, 1988b; Hall & Grose, 1988; Grose & Hall, 1989; Moore et al., 1990; Moore & Schooneveldt, 1990; Yost & Sheft, 1990; van den Brink, Houtgast, & Smoorenburg, 1992; Fantini, Moore, & Schooneveldt, 1993). One simple explanation for the increase in threshold holds that energy from the flanking bands physically masked the signal by leaking into the critical band centered on the signal frequency. For the phase-incoherent conditions, when the envelope amplitude of the 2500-Hz band is near a minimum, the amplitudes of the flanking band envelopes will be considerably greater. This is clearly demonstrated in the middle panels of Fig. 4-2. Assuming critical band filtering and the

proximity of the flanking bands, a certain amount of leakage is unavoidable.

Simulations

To test whether higher thresholds in the presence of incoherent flanking bands were due to direct masking, a series of simulations was conducted. The output of a simulated critical band filter centered at the signal frequency was calculated for various masker inputs, and the change in masker level for the multi-band maskers relative to the single-band masker was calculated and compared to corresponding threshold changes.

The critical band filter was simulated by a fourth-order GammaTone filter (Holdsworth, Nimmo-Smith, Patterson, & Rice, 1988) with a nominal half-power bandwidth corresponding to the ERB at the signal frequency, or 295 Hz (Glasberg & Moore, 1990). One important parameter of the simulations was the duration over which the masker levels were computed. In similar simulations, Moore et al. (1990) computed levels within a 10-ms window corresponding to either a peak or valley in their on-frequency band masker. This window was chosen as a reasonable approximation of the temporal resolution of the ear. A 10-ms window would be advantageous for valley signal placement because a minimal amount of masker energy would be integrated. For peak placement, however, a longer time window would give a more favorable masker level. In the present simulations, levels were calculated for integration windows ranging from 1 ms

to 50 ms, roughly corresponding to the temporal resolution of the ear and to the duration of the pulse-train signals.

For each modulated masker condition, the energy of the masker was integrated over a single cycle of modulation. The time constant of integration, τ, was nominally 1, 10, or 50 ms. The results of these simulations are given in Fig. 4-7 with the energy of the masker (10 log [Em]) plotted against time (sec) which spans one period of modulation, or 0.1 seconds. Each of the six panels corresponds to a different multi-band masker condition. Within a single panel there are six curves, corresponding to τ values of 1, 10, and 50 ms (as labeled in the lower left panel) for both the multi-band masker (dashed curves) and the appropriate single-band masker comparison (solid curves). Each curve is based upon 100 masker samples.

Consider the results in the PI/I panel (upper left). In this condition, the multi-band masker (dashed curves) is composed of five incoherent noise carriers (100-Hz wide) which have phase-incoherent amplitude modulation (10 Hz). Within the same panel, the solid curves are for a single-band amplitude modulated noise centered at 2500 Hz. For an integration time of 50 ms (upper curves), the single-band masker energy decreases only 8 dB from a masker peak (0.0 or 0.1 sec) to a masker valley (0.05 ms). In contrast, an integration time of 1 ms (lower curves) indicates a 60-dB change in masker energy from a peak to a valley of the masker. For the multi-band masker and τ = 50 ms, the

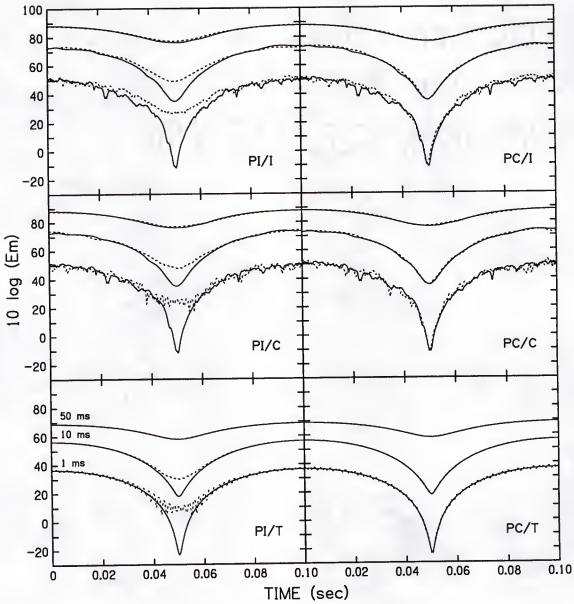

Figure 4-7. Masker energy versus time corresponding to one period of amplitude modulation. Each panel represents a different multi-band masker condition. In each panel, curves are shown for multi-band (dashed curves) and corresponding single-band (solid curves) masker conditions for three integration times: 50 ms (upper curves), 10 ms (middle curves), and 1 ms (lower curves). Each curve is based upon the average of 100 masker samples.

masker energy is nearly the same as for the single-band masker. In other words, the leakage from flanking maskers produces only a slight relative change in masker energy when averaged over this period. For τ = 1 ms, however, there is (40 dB) at a modulation minimum (0.05 sec). This indicates that if the auditory system actually integrated energy over a 1-ms time period, the masker energy at a valley would be much less in the single-band condition than the multi-band masker, or that substantial leakage could be detected.

It is interesting to compare these results with the PC/I condition, where the amplitude modulation is phase-coherent across the five masker bands. Here, the leakage from flanking bands should be negligible, as the masker peaks and valleys are the same across frequency. The three sets of curves in the PC/I panel (upper right) confirm this expectation. For each of the three τ values, the single-band and multi-band curves overlap, indicating essentially the same masker energy for both conditions. Similar results were obtained for the middle and lower two panels, where data for the coherent noise carriers (PI/C and PC/C) and the tonal carriers (PI/T and PC/T) are shown.

Now consider these simulations with respect to the actual masked pure-tone thresholds for each condition. Beginning with the PI/I condition, the actual threshold difference between the single-band masker and the phase-incoherent masker was 12.9 dB. To explain this difference

in terms of changes in masker energy, the integration time would certainly have to be somewhere between 50 ms, where the masker energy differed by less than 1 dB, and 1 ms, where the difference was about 40 dB. In fact, a time constant of 11 ms predicts the threshold difference of 12.9 dB. In other words, if one assumes an integration time of 11 ms, then the change in masked threshold from the single-band masker to the phase incoherent masker (PI/I) could be accounted for based entirely upon a leakage of energy from the flanking bands into the region surrounding the pure-tone signal.

Similar τ values were determined for the phase-incoherent conditions having coherent noise and tonal carriers. Integration times were calculated that would account for the actual threshold increases due to the presence of multiple flanking band maskers. Corresponding τ values were 13 and 11 ms for the coherent noise and tonal carriers, respectively.

Of course for the phase-coherent maskers (right-hand panels), there is little difference in masker energy between the single-band and multi-band conditions, regardless of τ value. As masked thresholds were substantially lower in the multi-band than the single-band conditions, indicating a **masking release**, these results cannot be explained in terms of changes in masking energy.

Similar values of τ were obtained for the pulse-train signals for valley signal placement (Exp. 3). Because

single-band minus multi-band threshold differences were slightly larger than for the 500-ms signal, assumed integration values were smaller for the pulse-train signals by 1 to 3 ms.

The simulations also indicate that changes in masking energy cannot explain the increase in masked threshold that occurred in all modulated conditions with peak signal placement (Exp. 3). This is clearly seen in Fig. 4-7, where single-band and multi-band maskers have essentially the same masker energy at a cycle peak (e.g. 0.0 and 0.10 sec). In this case, some form of interference or indirect masking must occur. Moore et al. (1990) termed this "across-channel masking."

Conclusions

The present data are largely consistent with a "cued temporal listening" strategy in which the coherent flanking bands cue the presence of envelope minima, where the best signal-to-noise ratio is available. Analyses indicate that an envelope correlation model similar to that proposed by Richards (1987) failed to account for thresholds reported here. The addition of flanking bands having envelopes that are incoherent with the single-band envelope lead to an increase in masking. Analyses indicating that the additional masking was due in part to "leakage" of energy from the flanking bands into the frequency region surrounding the signal. This leakage, however, could not account for

the entire masking effect. Some form of indirect masking or interference occurs as a result of incoherent flanking bands.

These experiments confirmed the importance of envelope fluctuation rate for comodulation masking release. CMR is maximal for low rates of envelope fluctuation and diminishes for higher rates. Provided with two rates of fluctuation simultaneously, obtained by amplitude modulating narrowband noise, CMR results from across channel coherence of either rate. When both rates are coherent across frequency, CMR is greater than either rate alone. These data suggest that the auditory system is able to use both envelope rates to make across-frequency envelope comparisons.

CHAPTER 5
CONCLUSIONS

The study of temporal processing is vital to a broader understanding of the capabilities of the auditory system and to the mechanisms underlying hearing. The present study dealt with two primary issues involved in auditory temporal processing: temporal acuity and across-frequency temporal processing. Temporal acuity, or the ability to detect changes in stimuli over time, is a fundamental property of audition and plays an important role in extracting information from the acoustic stimulus. Across-frequency temporal processing, as illustrated by comodulation masking release, can improve signal detection by resolving and comparing temporal patterns across different spectral regions.

Previous investigations of temporal acuity have failed to establish the influence of stimulus frequency region and stimulus bandwidth on measures of temporal acuity using noise stimuli. The second and third chapters of this study were devoted to this issue. In Chapter 2, temporal acuity was investigated using a modulation detection paradigm. By measuring the sensitivity to modulation as a function of modulation frequency using narrowband noise stimuli, a temporal modulation transfer function (TMTF) was obtained,

characterizing the temporal response of the auditory system. By varying the upper cutoff frequency of the narrowband noise and holding the noise bandwidth constant, it was determined that modulation detection was independent of stimulus frequency region over the range of 600 to 4400 Hz. Similarly, by varying the noise bandwidth while holding the stimulus frequency constant, it was determined that modulation detection improved with increasing noise bandwidth from 200 to >2000 Hz.

Measurements of modulation detection were essentially constant over a 50 dB range of stimulus levels for both narrowband and wideband noise, indicating that temporal acuity is constant over such a range. Additional measures of modulation detection in the presence of notched-noise masking demonstrated that similar TMTFs for low- and high-frequency stimuli in the previous experiments were not due simply to high-frequency auditory excitation by the low-frequency stimulus. This was consistent with finding that modulation detection was independent of stimulus frequency region. Finally, psychometric functions were obtained for modulation detection that were steeper as modulation frequency increased from 4 to 250 Hz and were essentially the same for different noise bandwidths and frequency regions.

Temporal acuity was also estimated using modified masking period patterns. In this paradigm, estimates of temporal acuity are based on the detection of a pure-tone signal masked by unmodulated or amplitude modulated noise.

Using the difference in threshold between the two masker types as a function of modulation frequency, a TMTF was derived. Similar to the modulation detection data, the results indicated that temporal acuity was independent of stimulus frequency for narrowband noise maskers.

The experiments in Chapter 4 employed a comodulation masking release (CMR) paradigm to investigate the role of envelope fluctuation rate in across-frequency temporal processing. Pure-tone signals were masked by stimuli having either incoherent or coherent stimulus envelopes across frequency. When the envelopes of the maskers remote from the signal were incoherent with the masker centered at the signal, detection was the same or worse than if the remote maskers were absent altogether. However, when the remote maskers had envelopes coherent with the masker at the signal frequency, detection improved substantially.

In the first experiment of Chapter 4, this release from masking, or comodulation masking release, was shown to be maximal for slow rates of envelope fluctuation and diminished with increasing envelope rate. In the final two experiments, maskers included amplitude modulated narrowband noise, for which two rates of envelope coherence could be obtained simultaneously. Resulting CMR values indicated that the auditory system could attend to a single coherent envelope rate, despite incoherence at the other rate. When both envelope rates were coherent across frequency, the CMR magnitude was greater than for either single rate alone.

These results were interpreted as favoring a "cued temporal listening" strategy for CMR in which stimulus envelopes remote from the signal cue the presence of masker minima, where signal detection is optimal. By placing more importance on the ratio of signal-to-masker energy at a masker minima, signal detection is improved with the presence of remote coherent-envelope maskers.

The results in Chapters 2 and 3 indicated that modulation detection and pure-tone detection in modulated noise are best at low modulation frequencies. These results are consistent with the experiments of Chapter 4, which showed the greatest CMR for low envelope fluctuation rates, thereby illustrating the importance of temporal acuity in processes underlying CMR.

APPENDIX
MODULATION DETECTION OF NARROWBAND NOISE: ANALOG VERSUS DIGITAL FILTERING

The improved modulation thresholds with increasing frequency region reported by van Zanten (1980) may be a result of the increase in "effective" signal bandwidth due to analog filtering. To test this hypothesis, modulation thresholds were measured using two methods of filtering. For one set of thresholds, filtering was accomplished using the digital filtering method of Exp. 1. For a second set of thresholds, noise was filtered with two analog filters (Krohn-Hite 3343) in series having a total attenuation of 96 dB/octave. Procedures and stimulus generation were identical to Exp. 1. Stimulus conditions included modulation frequencies of 8 and 64 Hz, upper cutoffs of 2200 and 4400 Hz, and a nominal bandwidth of 800 Hz. These conditions were chosen because they proved quite stable in Exp. 1. Threshold for a condition was taken as the average of three threshold runs. The results for one subject are shown in Table A-1. The threshold difference between the 2200- and 4400-Hz frequency regions was 0.6 dB for digital filtering. In contrast, for analog filtering, this difference was 3.0 dB. The standard error of the mean was 0.5 dB. The difference in filtering techniques may therefore account for differences in sensitivity to modulation

TABLE A-1. Modulation threshold vs modulation frequency at two frequency regions (2200 and 4400 Hz) using both digital and analog filtering. The third data column shows the threshold difference across frequency regions for the two filter conditions.

Upper cutoff freq.	fm	2200 Hz	4400 Hz	DIFF
Digital	8 Hz	16.5	17.0	0.5
	64 Hz	11.7	12.4	0.7
Analog	8 Hz	18.4	20.8	2.4
	64 Hz	14.1	17.7	3.6

reported here and by van Zanten. This difference reflects the influence of stimulus bandwidth rather than frequency region on modulation detection, as demonstrated in Exp. 1.

REFERENCES

Bacon, S. P., & Viemeister, N. F. (1985). Temporal modulation transfer functions in normal-hearing and hearing-impaired listeners. Audiology, 24, 117-134.

Buunen, T. J. F. (1976). On the perception of phase differences in acoustics. Unpublished doctoral dissertation, Technical University, Delft, The Netherlands.

Buus, S. (1985). Release from masking caused by envelope fluctuations. Journal of the Acoustical Society of America, 78, 1958-1965.

Buus, S., & Florentine, M. (1985). Gap detection in normal and impaired listeners: The effect of level and frequency. In A. Michelsen (Ed.), Time resolution in auditory systems (pp. 159-179). New York: Springer-Verlag.

Carlyon, R. P., Buus, S., & Florentine, M. (1989). Comodulation masking release for three types of modulator as a function of modulation rate. Hearing Research, 42, 37-46.

Cohen, M. F., & Schubert, E. D. (1987). The effect of cross-spectrum correlation on the detectability of a noise band. Journal of the Acoustical Society of America, 81, 721-723.

Cornsweet, T. M. (1970). Visual perception. New York: Academic Press.

De Boer, E. (1966). Intensity discrimination of fluctuating signals. Journal of the Acoustical Society of America, 40, 552-560.

Durlach, N. I. (1963). Equalization and cancellation theory of binaural masking-level differences. Journal of the Acoustical Society of America, 35, 1206-1218.

Eddins, D. A., & Green, D. M. (In Press). Temporal integration and temporal resolution. In B. C. J. Moore (Ed.), Handbook of perception and cognition, volume 6, hearing. New York: Academic Press.

Eddins, D. A., Hall, J. W., & Grose, J. H. (1992). The detection of temporal gaps as a function of frequency region and absolute stimulus bandwidth. Journal of the Acoustical Society of America, 91, 1069-1077.

Fantini, D. A., Moore, B. C. J., & Schooneveldt, G. P. (1993). Comodulation masking release as a function of type of signal, gated or continuous masking, monaural or dichotic presentation of flanking bands, and center frequency. Journal of the Acoustical Society of America, 93, 2106-2115.

Fitzgibbons, P. J. (1983). Temporal gap detection in noise as a function of frequency, bandwidth, and level. Journal of the Acoustical Society of America, 74, 67-72.

Fitzgibbons, P. J. (1984). Temporal gap resolution in narrow-band noises with center frequencies from 6000 to 14000 Hz. Journal of the Acoustical Society of America, 75, 566-569.

Fitzgibbons, P. J., & Wightman, F. L. (1982). Gap detection in normal and hearing-impaired listeners. Journal of the Acoustical Society of America, 72, 761-765.

Fletcher, H. (1940). Auditory Patterns. Review of Modern Physics, 12, 47-65.

Formby, C., & Forrest, T. G. (1991). Detection of silent temporal gaps in sinusoidal markers. Journal of the Acoustical Society of America, 89, 830-837.

Formby, C., Forrest, T. G., & Raney, J. J. (1992). Simulated modulation detection via an envelope detector model implemented with triangular-shaped peripheral filters and traditional filter bandwidths. Abstracts of the 15th midwinter meeting of the Association for Research in Otolaryngology, St. Petersburg, FL, p. 68.

Formby, C., & Muir, K. (1988). Modulation and gap detection for broadband and filtered noise signals. Journal of the Acoustical Society of America, 84, 545-550.

Forrest, T. G., & Green, D. M. (1987). Detection of partially filled gaps in noise and the temporal modulation transfer function. Journal of the Acoustical Society of America, 82, 1933-1943.

Glasberg, B. R., & Moore, B. C. J. (1990). Derivation of auditory filter shapes from notched-noise data. Hearing Research, 47, 103-138.

Glasberg, B. R., Moore, B. C. J., & Bacon, S. P. (1987). Gap detection and masking in hearing-impaired and normal-hearing subjects. Journal of the Acoustical Society of America, 81, 1546-1556.

Green, D. M. (1960). Auditory detection of a noise signal. Journal of the Acoustical Society of America, 32, 121-131.

Green, D. M. (1973a). Minimum integration time. In A. R. Møller (Ed.), Mechanisms in hearing (pp. 829-846). New York: Academic Press.

Green, D. M. (1973b). Temporal acuity as a function of frequency. Journal of the Acoustical Society of America, 54, 373-79.

Green, D. M. (1992). On the similarity of two theories of comodulation masking release. Journal of the Acoustical Society of America, 91, 1769.

Green, D. M., & Forrest, T. G. (1989). Temporal gaps in noise and sinusoids. Journal of the Acoustical Society of America, 86, 961-970.

Grose, J. H., Eddins, D. A., & Hall, J. W. (1989). Gap detection as a function of stimulus bandwidth with fixed high-frequency cutoff in normal-hearing and hearing-impaired listeners. Journal of the Acoustical Society of America, 86, 1747-1755.

Grose, J. H., & Hall, J. W. (1989). Comodulation masking release using SAM tonal complex maskers: Effects of modulation depth and signal position. Journal of the Acoustical Society of America, 85, 1276-1284.

Grose, J. H., Hall, J. W., & Gibbs, C. (1993). Temporal analysis in children. Journal of Speech and Hearing Research, 36, 351-356.

Haggard, M. P., Hall, J. W., & Grose, J. H. (1990). Comodulation masking release as a function of bandwidth and test frequency. Journal of the Acoustical Society of America, 88, 113-118.

Hall, J. W. (1986). Binaural frequency selectivity and CMR. In B. C. J. Moore & R. D. Patterson (Eds.), Frequency selectivity, (pp. 387-395). New York: Plenum Press).

Hall, J. W. (1987). Experiments on comodulation masking release. In W. A. Yost & C. S. Watson (Eds.), Auditory processing of complex sounds (pp. 57-66). Hillsdale, NJ: Erlbaum.

Hall, J. W. III, Cokely, J. A., & Grose, J. H. (1988). Combined monaural and binaural masking release. Journal of the Acoustical Society of America, 83, 1639-1845.

Hall, J. W., & Grose, J. H. (1988). Comodulation masking release: Evidence for multiple cues. Journal of the Acoustical Society of America, 84, 1669-1675.

Hall, J. W., Grose, J. H., & Moore, B. C. J. (1993). Influence of frequency selectivity on comodulation masking release in normal-hearing listeners. Journal of Speech and Hearing Research, 36, 410-423.

Hall, J. W., & Haggard, M. P. (1983). Co-modulation: a principle for auditory pattern analysis in speech. Proceedings of the 11th International Congress on Acoustics, 4, 69-71.

Hall, J. W., Haggard, M. P., & Fernandes, M. A. (1984). Detection in noise by spectro-temporal pattern analysis. Journal of the Acoustical Society of America, 78, 50-56.

Holdsworth, J., Nimmo-Smith, I., Patterson, R., & Rice, P. (1988). Implementing a GammaTone filter bank. Unpublished report.

Laming, D. (1986). Sensory analysis. New York: Academic Press.

Levitt, H. (1971). Transformed up-down methods in psychoacoustics. Journal of the Acoustical Society of America, 49, 467-477.

McFadden, D. (1986). Comodulation masking release: Effects of varying the level, duration, and time delay of the cue band. Journal of the Acoustical Society of America, 80, 1658-1667.

McFadden, D. (1987). Comodulation detection differences using noise-band signals. Journal of the Acoustical Society of America, 81, 1519-1527.

Moore, B. C. J., & Glasberg, B. R. (1988). Gap detection with sinusoids in normal, impaired, and electrically stimulated ears. Journal of the Acoustical Society of America, 83, 1093-1101.

Moore, B. C. J., Glasberg, B. R., Plack, C. J., & Biswas, A. K. (1989). Detection of temporal gaps in sinusoids by normally hearing and hearing-impaired subjects. Journal of the Acoustical Society of America, 85, 1266-1275.

Moore, B. C. J., Glasberg, B. R., & Schooneveldt, G. P. (1990). Across-channel masking and comodulation masking release. Journal of the Acoustical Society of America, 87, 1683-1694.

Moore, B. C. J., & Schooneveldt, G. P. (1990). Comodulation masking release as a function of bandwidth and time delay between on-frequency and flanking-band maskers. Journal of the Acoustical Society of America, 88, 725-731.

Plack, C. J., & Moore, B. C. J. (1990). Temporal window shape as a function of frequency and level. Journal of the Acoustical Society of America, 87, 2178-2187.

Plomp, R. (1964). Rate of decay of auditory sensation. Journal of the Acoustical Society of America, 36, 277-282.

Rice, S. O. (1954). Mathematical analysis of random noise. In N. Wax (Ed.), Selected papers on noise and stochastic processes (pp. 133-294). New York: Dover.

Richards, V. (1987). Monaural envelope correlation detection. Journal of the Acoustical Society of America, 82, 1621-1630.

Rodenburg, M. (1977). Investigation of temporal effects with amplitude modulated signals. In E. F. Evans & J. P. Wilson (Eds.), Psychophysics and Physiology of Hearing (pp. 429-437). London: Academic Press.

Schacknow, P. N., & Raab, D. H. (1976). Noise-intensity discrimination: effects of bandwidth conditions and mode of masker presentation. Journal of the Acoustical Society of America, 60, 893-905.

Schooneveldt, G. P., & Moore, B. C. J. (1987). Comodulation masking release (CMR) for as a function of signal frequency, flanking band frequency, masker bandwidth, and flanking band level. Journal of the Acoustical Society of America, 82, 1944-1956.

Schooneveldt, G. P., & Moore, B. C. J. (1988). Comodulation masking release for various monaural and binaural combinations of the signal, on-frequency, and flanking bands. Journal of the Acoustical Society of America, 85, 262-272.

Schooneveldt, G. P., & Moore, B. C. J. (1988). Comodulation masking release (CMR) as a function of masker bandwidth, modulator bandwidth, and signal duration. Journal of the Acoustical Society of America, 85, 273-281.

Shailer, M. J., & Moore, B. C. J. (1983). Gap detection as a function of frequency, bandwidth, and level. Journal of the Acoustical Society of America, 74, 467-473.

Shailer, M. J., & Moore, B. C. J. (1985). The detection of temporal gaps in bandlimited noise: Effects of variations in bandwidth and signal-to-masker ratio. Journal of the Acoustical Society of America, 77, 635-639.

Shailer, M. J., & Moore, B. C. J. (1987). Gap detection and the auditory filter: Phase effects using sinusoidal stimuli. Journal of the Acoustical Society of America, 81, 1110-1117.

Spiegel, M. F. (1981). Thresholds for tones in maskers of various bandwidths and for signals of various bandwidths as a function of signal frequency. Journal of the Acoustical Society of America, 69, 791-795.

van den Brink, W. A. C., Houtgast, T., & Smoorenburg, G. F. (1992). Signal detection in temporally modulated and spectrally shaped maskers. Journal of the Acoustical Society of America, 91, 267-278.

van Zanten, G. A. (1980). Temporal modulation transfer functions for intensity modulated noise bands. In G. van den Brink & F. A. Bilsen (Eds.), Psychophysical and behavioral studies in hearing (pp. 206-209). Delft, The Netherlands: Delft University Press.

Viemeister, N. F. (1977). Temporal factors in audition: a systems analysis approach. In E. F. Evans & J. P. Wilson (Eds.), Psychophysics and physiology of hearing (pp. 419-427). London: Academic Press.

Viemeister, N. F. (1979). Temporal modulation transfer functions based upon modulation thresholds. Journal of the Acoustical Society of America, 66, 1364-1380.

Weber, D. L. (1977). Integration time and temporal modulation transfer function in auditory detection. Unpublished doctoral dissertation, Harvard University, Cambridge.

Wier, C., Jesteadt, W. , & Green, D. M. (1977). Frequency discrimination as a function of frequency and sensation level. Journal of the Acoustical Society of America, 61, 178-184.

Yost, W. A., & Sheft, S. S. (1990). A comparison among three measures of cross-spectral processing of amplitude modulation with tonal signals. Journal of the Acoustical Society of America, 87, 897-900.

Zwicker, E. (1980). A device for measuring the temporal resolution of the ear. Audiological Acoustics, 19, 2-12.

Zwicker, E., & Schorn, K. (1982). Temporal resolution in hard of hearing patients. Audiology, 21, 474-492.

Zwislocki, J. (1960). Theory of auditory temporal summation. Journal of the Acoustical Society of America, 26, 1046-1060.

BIOGRAPHICAL SKETCH

David A. Eddins, born in Raleigh, North Carolina, on October 12, 1964, is the son of John W. Eddins, Jr., and the late Joanne H. Eddins. He graduated from Millbrook Senior High School in 1982. David received an A. B. in speech and hearing sciences in 1986 and a M.S. in audiology in 1988 from the University of North Carolina. As a graduate student at UNC, he was a research assistant in the Psychoacoustics Laboratory of Joseph W. Hall. While studying under Dr. Hall, David's career goals focused on a combination of the fields of audiology and psychoacoustics. David then took a position as a clinical fellow-research assistant in audiology at the Veterans Administration Hospital in Long Beach, California. After obtaining clinical certification in audiology, David returned to NC in January, 1990 and worked as a research audiologist in the Psychoacoustics Laboratory. In August of that year, he enrolled in the doctoral program in psychology at the University of Florida, where he worked under the supervision of David M. Green. David plans a career in academia and hopes to continue to study the auditory system in normal-hearing and hearing-impaired listeners.

I certify that I have read this study and that in my opinion it conforms to acceptable standards of scholarly presentation and is fully adequate, in scope and quality, as a dissertation for the degree of Doctor of Philosophy.

David M. Green, Chair
Graduate Research Professor
of Psychology

I certify that I have read this study and that in my opinion it conforms to acceptable standards of scholarly presentation and is fully adequate, in scope and quality, as a dissertation for the degree of Doctor of Philosophy.

Robert D. Sorkin
Professor of Psychology

I certify that I have read this study and that in my opinion it conforms to acceptable standards of scholarly presentation and is fully adequate, in scope and quality, as a dissertation for the degree of Doctor of Philosophy.

W. Keith Berg
Professor of Psychology

I certify that I have read this study and that in my opinion it conforms to acceptable standards of scholarly presentation and is fully adequate, in scope and quality, as a dissertation for the degree of Doctor of Philosophy.

Elizabeth D. Capaldi
Professor of Psychology

I certify that I have read this study and that in my opinion it conforms to acceptable standards of scholarly presentation and is fully adequate, in scope and quality, as a dissertation for the degree of Doctor of Philosophy.

John C. Middlebrooks
Associate Professor
of Neuroscience

This dissertation was submitted to the Graduate Faculty of the Department of Psychology in the College of Liberal Arts and Sciences and to the Graduate School and was accepted as partial fulfillment of the requirements for the degree of Doctor of Philosophy.

August, 1993

_____

Dean, Graduate School